COMBINATORIAL PROOF FOR THE RATIONALITY OF THE BIVARIATE GENERATING SERIES OF MAPS IN POSITIVE GENUS

MARIE ALBENQUE AND MATHIAS LEPOUTRE

ABSTRACT. In this paper, we give the first combinatorial proof of a rationality scheme for the generating series of maps in positive genus enumerated by both vertices and faces, which was first obtained by Bender, Canfield and Richmond in 1993 by purely computational techniques.

To do so, we rely on a bijection obtained by the second author in a previous work between those maps and a family of decorated unicellular maps. Our main contribution consists in a fine analysis of this family of maps. As a byproduct, we also obtain a new and simpler combinatorial proof of the rationality scheme for the generating series of maps enumerated by their number of edges, originally obtained computationally by Bender and Canfield in 1991 and combinatorially by the second author in 2019.

1. Introduction

This article deals with the enumerative properties of maps of genus g. Informally, a map of genus g is a proper embedding of a graph on a g-hole torus. Maps of genus 0 – also called $planar\ maps$ – were first studied by Tutte in the 60's. In a series of papers, he developed a robust method that allowed him to obtain many enumerative results, through the resolution of generating series obtained by a combinatorial decomposition [20, 21]. Since then, the enumeration of maps has been studied extensively in various fields of mathematics and mathematical physics; other classical techniques to enumerate maps include matrix integrals, topological recursion and bijection with decorated trees (see for instance [13], [11], [19] and references therein).

The first enumerative results for maps on surfaces of positive genus were obtained by Lehman and Walsh [22, 23], who gave expressions for the generating series of maps with fixed excess (the excess is the difference between the number of edges and the number of vertices minus 1). Then, Bender and Canfield combined the method developed by Tutte together with some fine manipulation of recurrence relations on the generating functions to obtain first the asymptotic behavior of maps of a given genus enumerated by edges [4]. For $g \ge 0$, denote by \mathcal{M}_g the set of rooted maps of genus g and denote $M_g(z)$ their following generating series:

$$M_g(z) = \sum_{\mathfrak{m} \in \mathcal{M}_g} z^{|E(\mathfrak{m})|}, \quad \text{ where } E(\mathfrak{m}) = \{\text{edges of } \mathfrak{m}\}.$$

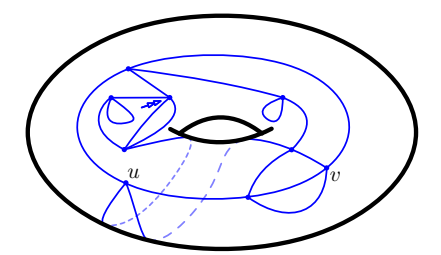
Then, in [5], they refined their result to obtain closed formulas for $M_1(z)$, $M_2(z)$ and $M_3(z)$. But, more importantly, they exhibited the following rationality scheme:

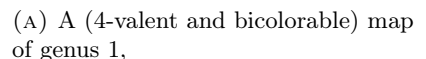
Theorem 1.1 (Tutte [21] for g = 0, Bender and Canfield [5] for $g \ge 1$). Let T(z) be the unique formal power series in z that satisfies $T(z) = z + 3T^2(z)$ and T(0) = 0. Then, for any $g \ge 0$, $M_g(z)$ is a rational function of T(z).

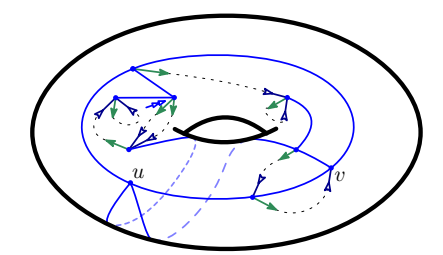
Though the number of maps with a fixed genus and a fixed number of edges is finite, this is not the case for maps with a fixed genus and a fixed number of vertices (or a fixed number of faces). But, in view of Euler's formula, which states that for any map \mathfrak{m} of genus g:

$$|V(\mathfrak{m})| + |F(\mathfrak{m})| = 2 - 2q + |E(\mathfrak{m})|,$$

(where $F(\mathfrak{m})$ and $V(\mathfrak{m})$ denote respectively the set of faces and of vertices of \mathfrak{m}), a natural way to refine the result of Bender and Canfield is to count maps by both their number of vertices and their number of faces. Hence, for any fixed $g \geq 1$, define $M_g(z_{\bullet}, z_{\circ})$ to be the generating series of







(B) and its corresponding spanning decorated unicellular map.

FIGURE 1. Illustration of the bijection of [14] for a 4-valent map on a torus of genus 1.

We associate to a map (represented in (A) one of its spanning unicellular submaps decorated by some opening and closing half-edges (respresented in (B). These half-edges can be matched as in a parenthis word to reconstruct the facial cycles.

rooted maps of genus g enumerated by both their vertices and faces, i.e.:

$$M_g(z_{\bullet}, z_{\circ}) = \sum_{\mathfrak{m} \in \mathcal{M}_g} z_{\bullet}^{|V(\mathfrak{m})|} z_{\circ}^{|F(\mathfrak{m})|}.$$

Arquès obtained the first results in this direction and gave explicit formulae for M_0 and M_1 in [1, 2]. Then, in [6], Bender, Canfield and Richmond refined Theorem 1.1 and obtained the following bivariate rationality scheme:

Theorem 1.2 (Arquès [1, 2] for g = 0, 1, Bender, Canfield and Richmond [6] for $g \ge 2$). Define $T_{\bullet}(z_{\bullet}, z_{\circ})$ and $T_{\circ}(z_{\bullet}, z_{\circ})$ as the unique formal power series with constant term equal to 0 and that satisfy

(1)
$$\begin{cases} T_{\bullet} = z_{\bullet} + T_{\bullet}^{2} + 2T_{\circ}T_{\bullet} \\ T_{\circ} = z_{\circ} + T_{\circ}^{2} + 2T_{\circ}T_{\bullet} \end{cases}$$

Then $M_q(z_{\bullet}, z_{\circ})$ is a rational function of T_{\bullet} and T_{\circ} .

Since the formal power series T, T_{\circ} and T_{\bullet} appearing in Theorems 1.1 and 1.2 can naturally be interpreted as the generating series of some decorated trees, the rationality schemes obtained in Theorems 1.1 and 1.2 call for a combinatorial explanation. By that, we mean a decomposition of rooted maps into simple objects – enumerated by a rational generating function – onto which are glued the trees enumerated by either T or by T_{\circ} and T_{\bullet} .

The quest for combinatorial proofs of enumerative results obtained for maps has already quite a long history. The first bijection between planar maps and some trees was obtained by Cori and Vauquelin in [9]. It gave as an enumerative corollary Tutte's enumeration formula for planar maps. But, the real breakthrough came with major results obtained by Schaeffer [17, 18] who obtained two families of bijections between planar maps and some decorated trees. Since then, those bijections have been extended and generalized and it is now customary to call the first one a blossoming bijection and the second one a mobile-type bijection (a term first coined in [?]). In a blossoming bijection, the decorated tree associated to a map is one of its spanning trees with some decorations, which permit to reconstruct its facial cycles. In a mobile-type bijectionm, the tree is not necessarily spanning and its vertices carry some integral labels which encode some metric properties of the map. In the original works of Schaeffer, it was also proved that both these bijections provide a combinatorial explanation fo Tutte's enumeration formula. Moreover, it is noteworthy for our purpose that the bijection obtained in [17] allows to get a combinatorial proof of the bivariate enumeration of planar maps (i.e. the case g = 0 in Theorem 1.2).

To get combinatorial proofs of Theorems 1.1 and 1.2, it is hence natural to try and generalize those bijections to higher genus. The natural analogue of trees in higher genus being unicellular

maps (i.e. maps with only one face), we hence aim at bijections between maps of genus g and decorated unicellular maps of genus g, rather than decorated plane trees.

In [8], Chapuy, Marcus and Schaeffer extended the bijection of [18], and thus obtained a mobile-type bijection for maps in higher genus. But, unfortunately, it did not give a combinatorial proof of the rationality scheme obtained in [5], but only of a slightly weaker version of it. In [14], the second author managed to extend Schaeffer's blossoming bijection of [17] to any genus, see Figure 1. And, by analyzing the decorated unicellular maps obtained via this construction, he was able to give a fully combinatorial proof of Theorem 1.1.

The purpose of this article is to give a *combinatorial proof* of Theorem 1.2, based on the same bijection. Let us first mention that (as in all the works aforementioned) we do not study directly general maps. Rather, we rely on the radial construction – introduced by Tutte [21] and recalled in Section 2.3 – which gives a bijection between maps and 4-valent maps, the faces of which can be properly bicolored in black and white (also called bicolorable 4-valent maps). It turns out that via this bijection, the number of vertices and of faces of the original map are sent to the number of black and white faces of its image.

Two main difficulties arise in the bivariate analysis of the unicellular maps obtained by applying the bijection of [14] to 4-valent bicolorable maps. First, an operation on unicellular maps (a.k.a. the rerooting procedure), which is critical to enumerate them, does not behave well when applied to a single map. But, we manage to prove that its effect is somehow balanced when applied to a whole subset of maps. This is the purpose of Theorem 3.11. In particular, as far as we are aware, this type of results is not available for mobile-type bijections and explains why the bijection obtained in [18] and its generalization to higher genus given in [8] fail to obtain bivariate enumerative corollary.

Secondly, the method developed in [14] to analyze unicellular blossoming maps cannot be extended to the bivariate enumeration. We developed here a new method, by proving some refined rationality schemes for subsets of unicellular blossoming maps. As a corollary, we obtain a new (and easier) proof of the original result of [14]. Let us be slightly more specific. The main reason why the bijection of [14] yields a combinatorial proof of Theorem 1.1 is the following. Define (informally) the scheme of a unicellular map as the map obtained by removing iteratively vertices of degree 1 and 2 (precise definitions of the scheme will be given later in Section 2.4). Then, the generating series of unicellular blossoming maps obtained by the bijection and with a prescribed scheme are also rational functions in terms of the series T defined in Theorem 1.1. It turns out that an analogous statement also holds for the bivariate generating series of unicellular maps with a prescribed scheme, which is rational in terms of T_{\bullet} and T_{\circ} defined in Theorem 1.2. What we prove precisely, which is stated in Theorem 5.11, is an even more refined rationality scheme for unicellular maps which share the same scheme and some other properties.

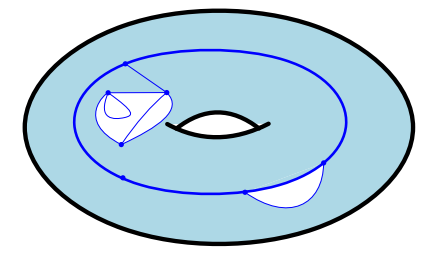
Our result hence confirms that, in higher genus, blossoming bijections produce the right "elementary objects", and demonstrates the robustness of blossoming bijections. Another illustration of their robustness is also its recent generalization to maps on non-orientable surfaces obtained by Maciej Dolęga and the second author in [10], which relies for some parts on an earlier version of the present work published in the PhD thesis of the second author [?, Chapter II.2].

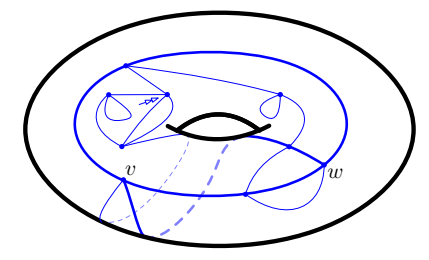
Let us conclude this introduction on a related note about the bivariate enumeration of maps. In [6], the authors obtained in fact a more precise result that Theorem 1.2 only and gave a general formula for M_g in terms of T_{\bullet} and T_{\circ} . This formula was precise enough to deduce the asymptotic enumeration of maps of genus g. Their formula (further simplified by Arquès and Giorgetti in [3]) is given below:

Theorem 1.3 ([6, 3]). For any fixed $g \ge 1$, $M_q(z_{\bullet}, z_{\circ})$ has the following form:

$$M_g(z_{\bullet}, z_{\circ}) = \frac{T_{\bullet}T_{\circ}(1 - T_{\bullet} - T_{\circ})P_g(T_{\bullet}, T_{\circ})}{\left((1 - 2T_{\bullet} - 2T_{\circ})^2 - 4T_{\bullet}T_{\circ}\right)^{5g - 3}},$$

where T_{\bullet} and T_{\circ} are the generating series defined in (1), and $P_g(x,y)$ is a symmetric polynomial with integer coefficients, of total degree not greater than 6g - 6.





(A) A graph embedded on the torus.

(B) A (4-valent) map of genus 1.

FIGURE 2. Two embeddings of a connected graph on the torus of genus 1. On (A), the embedding is not cellular: the shaded face is indeed not homeomorphic to a disk. On (B), the embedding is cellular and defines a map of genus 1.

A much more recent result about the bivariate enumeration of maps was given by Carrell and Chapuy [7]. Using the so-called KP-hierarchy, they obtain very nice recurrence relations for the number of maps with given genus and given number of vertices and faces, which (taking as an input the rationality result of Theorem 1.1) allows them to compute very efficiently the coefficients of the polynomial P_q appearing in Theorem 1.3.

Organization of the article: Section 2 is dedicated to introducing the terminology. We introduce the necessary material about bicolorable maps and orientations. In Section 3, we describe the closure operation, and prove in Theorem 3.11 that we can carry out the bivariate enumeration of unicellular blossoming maps even after some rerooting steps. In Section 4, we study the bivariate series of some Motzkin paths naturally appearing in Section 3, so as to prove, in Lemma 4.3, that the rationality stated in Theorem 1.2 amounts to the symmetry of a certain generating function. In Section 5, we focus on the generating series of unicellular maps refined by their scheme and some other statistics and state in Theorem 5.11, the refined rationality scheme that is key in our combinatorial proof of Theorem 1.1. We finally prove this theorem, first in Section 6 for the universate scheme, thus improving the proof [14], and then in Section 7 for the bivariate case, concluding the bijective proof of the rationality expressed in Theorem 1.2.

Acknowledgment: Both authors warmly thank Éric Fusy for suggesting this problem. Both authors were partially supported by the French ANR grant GATO (16 CE40 0009).

2. Notations, definitions and first constructions

2.1. **Notations.** In this article, combinatorial families are named with calligraphic letters (e.g. \mathcal{M}), their generating series in the corresponding capital letter (e.g. M(z)), and an object of the family is usually denoted by the corresponding lower case letter in gothic font (e.g. \mathfrak{m}).

For $n \in \mathbb{N}^*$, we set $[n] = \{1, \ldots, n\}$, and for $i, j \in \mathbb{N}$, with $i \leq j$, we set $[i, j] = \{i, \ldots, j\}$.

2.2. **Maps.** An *embedded graph* is a proper embedding of a connected graph on a surface, considered up to orientation-preserving homeomorphisms. A *face* of an embedded graph is a connected component of its complementary in the surface. An embedded graph is a *map* if all its faces are topologically equivalent to disks, see Figure 2. In this work we only consider maps on compact orientable surfaces without borders, which can be classified by their genus. The *genus* of a map is hence defined as the genus of its underlying surface.

For a map \mathfrak{m} , we denote respectively $V(\mathfrak{m})$, $E(\mathfrak{m})$ and $F(\mathfrak{m})$, its set of vertices, edges and faces.

An edge can be seen as the reunion of two *half-edges*, such that the removal of the middle point of an edge separates the two half-edges. The *degree* of a vertex is the number of half-edges adjacent to it. Equivalently, it is the number of edges adjacent to this vertex, with multiplicity. Similarly, the *degree* of a face is the number of edges adjacent to this face, with multiplicity.

The embedding fixes the cyclical order of edges around each vertex, which defines readily a *corner* as a couple of consecutive edges around a vertex. Corners may also be viewed as incidences

between vertices and faces. More precisely, a *corner* is an ordered pair (h, h'), where h and h' are two half-edges adjacent to the same vertex v such that h' directly follows h in counterclockwise order around v^1 . The set of corners of a map \mathfrak{m} is denoted $C(\mathfrak{m})$. For $\kappa \in C(\mathfrak{m})$, we denote by $v(\kappa)$ the vertex incident to κ .

A map \mathfrak{m} is rooted by marking one of its corners, which is called the root corner and denoted $\rho_{\mathfrak{m}}$ or ρ is there is no ambiguity. In figures, the root corner is indicated by a double arrow, see Figure 2(B). The vertex and the face incident to $\rho_{\mathfrak{m}}$ are respectively called the root vertex and the root face and are respectively denoted $v(\rho)$ and f_{ρ} .

2.3. Bicolorable maps and the radial construction. A map is called *bicolorable* if its faces can be properly colored with two colors, where a coloring is said to be proper if all the edges of the map separate faces of distinct colors². It is easy to see that a bicolorable map admits only two proper colorings of its faces, and that one is obtained one from the other by switching the color of every face.

Convention 1. In the following, all the rooted bicolorable maps are assumed to be properly colored in black and white with their root face being black, see Figure 3(B). With this convention, for \mathfrak{m} a rooted bicolorable map, we denote respectively $F_{\bullet}(\mathfrak{m})$ and $F_{\circ}(\mathfrak{m})$ the set of black and white faces of \mathfrak{m} .

Fix \mathfrak{m} a bicolorable map. The existence of a proper bicoloring implies immediately that for any $v \in V(\mathfrak{m})$, the degree of v is even. Therefore, a bicolorable map is Eulerian. In genus 0, a map is Eulerian if and only if it is bicolorable (and Schaeffer's original paper deals indeed with Eulerian planar maps). But this equivalence fails in positive genus, where some Eulerian maps may not be bicolorable, see for instance Figure 4(c). And, it appears that the right family of maps to consider in order to generalize Schaeffer's construction is the family of bicolorable maps rather than Eulerian maps.

We denote by \mathcal{BC}_g the set of bicolorable maps of genus g, and introduce their generating series BC_g when enumerated by both their number of black and white faces and by their degree distribution. More precisely, we set:

$$BC_g(z_\bullet,z_\circ;d_1,d_2,\ldots;t) = \sum_{\mathfrak{m}\in\mathcal{BC}_g} t^{|E(\mathfrak{m})|} z_\bullet^{|F_\bullet(\mathfrak{m})|} z_\circ^{|F_\circ(\mathfrak{m})|} \prod_{i\geq 1} d_i^{n_i(\mathfrak{m})},$$

where, for each $i \geq 1$, $n_i(\mathfrak{m})$ denotes the number of vertices of degree 2i of \mathfrak{m} . For $\mathfrak{m} \in \mathcal{BC}_g$, we clearly have $\sum_i i n_i(\mathfrak{m}) = |E(\mathfrak{m})|$, so that by Euler's formula:

$$|F_{\bullet}(\mathfrak{m})|+|F_{\circ}(\mathfrak{m})|=2-2g+\sum_{i\geq 1}(i-1)n_i(\mathfrak{m}).$$

This implies that BC_g is a formal power series in z_{\bullet} and z_{\circ} with polynomial coefficients in t and the d_i .

A map is said to be 4-valent if all its vertices have degree 4. The set of 4-valent bicolorable maps of genus g is denoted \mathcal{BC}_g^{\times} . Its bivariate generating series is denoted by $BC^{\times}(z_{\bullet}, z_{\circ})$, and corresponds to the following specialization:

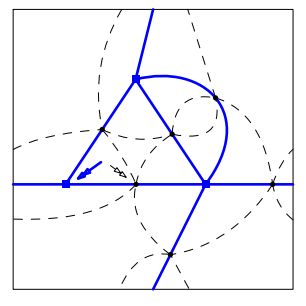
$$BC_q^{\times}(z_{\bullet}, z_{\circ}) = BC_g(z_{\bullet}, z_{\circ}; 0, 1, 0 \dots; 1),$$

which is indeed a formal power series in z_{\bullet} and z_{\circ} by the remark above.

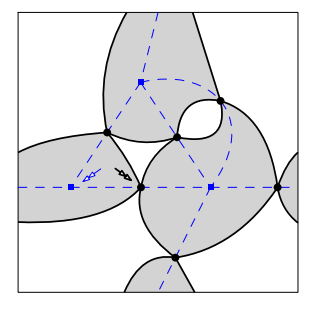
This family of maps holds special interest thanks to the radial construction introduced by Tutte in [21]. This construction maps bijectively \mathcal{M}_g to \mathcal{BC}_g^{\times} in the following way (illustrated in Figure 3). Fix $m \in \mathcal{M}_g$. The radial \mathfrak{r} of \mathfrak{m} is then defined as follows. First, the vertices of \mathfrak{r} correspond to the edges of \mathfrak{m} . Then, each corner of \mathfrak{m} gives rise to an edge in \mathfrak{r} . More precisely, for $(h, h') \in C(\mathfrak{m})$, let $e, e' \in E(\mathfrak{m})$ be such that $h \subset e$ and $h' \subset e'$. Write v_e and $v_{e'}$ for the

¹Note that, the embedding of the map (up to orientation-preserving homeomorphisms) is completely characterized by the cyclic ordering of the edges around each vertex. This fact will come in handy in the following as it allows us to represent maps without the underlying surface.

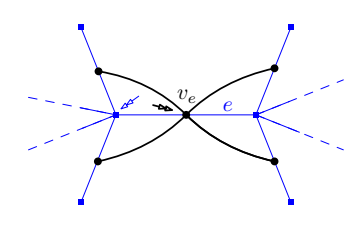
²The dual of bicolorable maps are bipartite maps which are more often encountered in the literature



(A) A map (plain edges) and its radial (dashed edges).



(B) A map (dashed edges) and its radial (plain edges).



(C) The local rule and the rooting convention

FIGURE 3. Illustration of the radial construction. The original map is represented with blue edges and square vertices and its radial by black edges and round vertices.

In (A) and (B), we use the classical representation of the torus of genus 1 as a square where both pairs of its opposite sides must be identified. In (B), the faces of the radial map are colored in black (actually gray for sake of visibility) and white, following our coloring convention.

corresponding vertices in \mathfrak{r} and add an edge in \mathfrak{r} between v_e and $v_{e'}$. Finally, we root \mathfrak{r} at the corner adjacent to the face f corresponding to the root vertex of \mathfrak{m} , and just after the edge of \mathfrak{r} corresponding to $\rho_{\mathfrak{m}}$, in clockwise order around f.

It can be proved that \mathfrak{r} is a map of genus g. Moreover, since every edge of \mathfrak{m} is incident to 4 corners, \mathfrak{r} is 4-valent. Faces of \mathfrak{r} correspond either to a vertex or a face of \mathfrak{m} . For $c \in C(\mathfrak{m})$, the corresponding edge of \mathfrak{r} separates the faces of \mathfrak{r} corresponding to the vertex and to the face adjacent to c. By consequence, \mathfrak{r} is bicolorable and the rooting convention ensures that vertices and faces of \mathfrak{m} correspond respectively to black and white faces of \mathfrak{r} . Hence, the radial construction has the following enumerative corollary, which is essential to our result:

Proposition 2.1 (radial map). The radial construction is a bijection between \mathcal{M}_g and \mathcal{BC}_g^{\times} . Moreover, fix $\mathfrak{m} \in \mathcal{M}_g$ and denote by \mathfrak{r} its image. Then, the radial construction induces a bijection between $V(\mathfrak{m})$ and $F_{\bullet}(r)$ on one hand and between $F(\mathfrak{m})$ and $F_{\circ}(r)$ on the other hand.

Therefore, it yields the following equality of generating series:

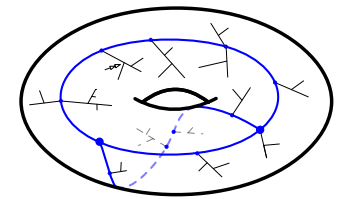
$$M_q(z_{\bullet}, z_{\circ}) = BC_q^{\times}(z_{\bullet}, z_{\circ})$$

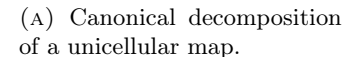
2.4. Unicellular maps, cores, schemes. A unicellular map is a map with only one face. In particular, a unicellular map of genus 0 is a plane tree.

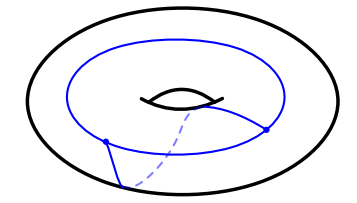
The *clockwise contour* of a unicellular map is the sequence of corners encountered while following the boundary of its unique face starting from its root corner, while keeping the interior of the face on its right. It corresponds to following the boundary of the disk homeomorphic to the face in clockwise direction, and note that it means turning in *counterclockwise* direction around the vertices.

The core of a unicellular map \mathfrak{u} – denoted $\Psi(\mathfrak{u})$ – is the map obtained from \mathfrak{u} by removing iteratively its vertices of degree one together with their incident edges. It is easy to see that the collection of deleted edges forms a forest of plane trees. Hence, a unicellular map can be canonically decomposed into its core and this forest of plane trees, see Figure 4(A). The operation of taking the core of \mathfrak{u} is called the *pruning* of \mathfrak{u} .

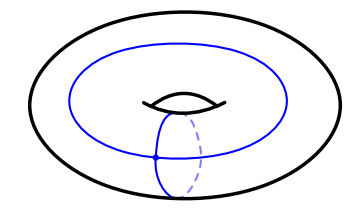
Next, the scheme of $\mathfrak u$ – denoted $\Theta(\mathfrak u)$ – is the map obtained from $\Psi(\mathfrak u)$ by additionally removing its vertices of degree 2. More precisely, for any v a vertex of degree 2 in $\Psi(\mathfrak u)$, denote by x,y be its two neighbours. Then, merge the two former edges $\{v,x\}$ and $\{v,y\}$ into an edge $\{x,y\}$ and delete v, see Figure 4(B).







(B) The scheme of genus 1 with 2 vertices.



(C) The scheme of genus 1 with 1 vertex.

FIGURE 4. In (A), we represent schematically the decomposition of a unicellular map into a forest of trees (represented in thin black edges) and a core (represented in fat blue edges). Its scheme is represented in (B). And in (C), we represent the other possible scheme of genus 1.

By extension, a *core* is a unicellular map in which all the vertices have degree not smaller than 2 and a *scheme* is a unicellular map in which all the vertices have degree not smaller than 3.

Remark 2.1. A simple computation shows that in genus 1, a scheme has either 1 or 2 vertices. Both possibilities are illustrated in Figure 4(B) and 4(C). When the scheme of a unicellular map $\mathfrak u$ of genus 1 has 2 vertices, it is convenient to represent $\mathfrak u$ inside an hexagon whose edges need then to be identified. In that case, the vertices of the hexagon correspond to the vertices of $\Theta(\mathfrak u)$. By extension, maps of genus 1 are often represented inside an hexagon: for instance the map represented in Figure 5 is the same as the one represented in Figure 2(B).

2.5. Orientations. An orientation of a map is an orientation of all its edges. An oriented map is a map endowed with an orientation. For the remainder of the section, let \mathfrak{m} be a fixed oriented map. A face of \mathfrak{m} is said to be clockwise (resp. counterclockwise) if its boundary forms a directed cycle such that $\rho_{\mathfrak{m}}$ lies on its left (resp. on its right).

Definition 2.2. The orientation of \mathfrak{m} is bicolorable if along any simple oriented loop ℓ drawn on the underlying surface such that $\ell \cap V(\mathfrak{m}) = \emptyset$, there are as many edges (with multiplicity) crossing ℓ towards its right and towards its left.

It is not difficult to see that if a map admits a bicolorable orientation, then it is bicolorable. Indeed, the existence of a bicolorable orientation implies directly that any cycle in the dual map has even length. Hence the dual map is bipartite, which implies that $\mathfrak m$ is bicolorable. In fact, reciprocally, any bicolorable map does admit one bicolorable orientation. We now describe one such orientation which will be quintessential to our work.

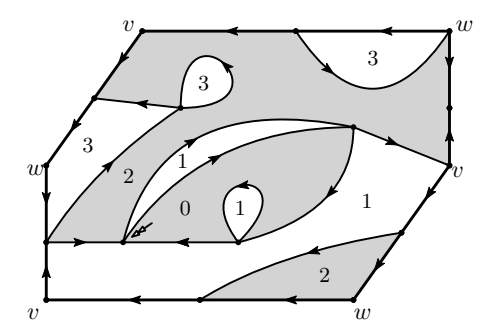
First, define the height function $h: F(\mathfrak{m}) \to \mathbb{N}$ of \mathfrak{m} as the unique function that satisfies the following conditions:

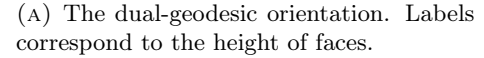
- The height of the root face is equal to 0,
- The height of a non-root face is equal to the minimum of the height of its adjacent faces plus 1.

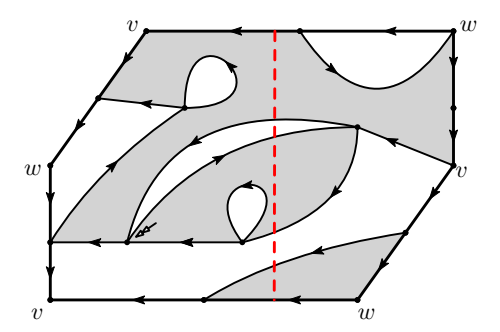
Note that for $f \in F(\mathfrak{m})$, h(f) can equivalently be defined as the dual distance between f and the root face. Note also that in the canonical coloring of the faces of a bicolorable map, black and white faces have respectively even and odd height, see Figure 5(A). Since \mathfrak{m} is bicolorable, the heights of two adjacent faces differ exactly by 1. Then, the *dual-geodesic orientation* of \mathfrak{m} is defined as the orientation such that the face on the left of an edge is the face with smaller height. It is clearly a bicolorable orientation.

The rest of this section is not directly used in this article. However, since it is crucial to the proof of [14, Theorem 3.14] on which relies heavily Theorem 3.7, we include it here for sake of completeness.

It is easy to see that a bicolorable map endowed with its dual-geodesic orientation has no clockwise face. The following theorem stated in [14, Corollary 2.19], and which is a consequence of the







(B) The orientation is not bicolorable as witnessed by the red dashed cycle.

FIGURE 5. The same 4-valent bicolorable map endowed with some Eulerian orientations with no clockwise face. The one in (A) is bicolorable and corresponds to the dual-geodesic orientation, the one in (B) is not bicolorable.

more general work of Propp [16], gives another characterization of the dual-geodesic orientation, based on this observation:

Theorem 2.3. For any bicolorable map, its dual-geodesic orientation is its unique bicolorable orientation with no clockwise face.

Remark 2.2. Consider a map \mathfrak{m} , endowed with a bicolorable orientation. Fix $v \in V(\mathfrak{m})$ and consider a small loop ℓ drawn on the underlying surface. The definition of a bicolorable orientation implies that half the edges incident to v are oriented towards it and half of them are oriented outwards it. This is precisely the definition on an Eulerian orientation. Therefore, any bicolorable orientation is in particular Eulerian.

The dichotomy between Eulerian and bicolorable orientations is reminiscent of the dichotomy between Eulerian and bicolorable maps. In genus 0, any Eulerian orientation is bicolorable. However, this is not true anymore in higher genus, see for instance Figure 5(B). The existence of the nice characterization of bicolorable orientations stated in Theorem 2.3 justifies the fact that bicolorable orientations are nicer to work with in higher genus.

3. BIJECTION FOR HIGHER-GENUS MAPS, COUNTING VERTICES AND FACES

3.1. **Definition of blossoming maps.** A blossoming map is a map \mathfrak{m} , with some additional unmatched half-edges, called *stems*. The set of stems is denoted $S(\mathfrak{m})$. For $s \in S(\mathfrak{m})$, we denote v(s) its incident vertex. Stems are oriented, and a stem s is called a *leaf* if it is oriented towards v(s) and a *bud* otherwise. The blossoming maps we consider have almost always as many buds as leaves.

The interior map $\mathring{\mathfrak{m}}$ of \mathfrak{m} is the map induced by $E(\mathfrak{m})$. For v a vertex of \mathfrak{m} , the *interior degree* of v – denoted $d\mathring{\mathrm{eg}}(v)$ – is the degree of v in $\mathring{\mathfrak{m}}$. An orientation of a blossoming map \mathfrak{m} is an orientation of $E(\mathfrak{m}) \cup S(\mathfrak{m})$.

Convention 2. A rooted blossoming map is always rooted in a corner that precedes (in counter-clockwise order) a bud. Equivalently, a rooted blossoming map is a blossoming map with a marked bud, called the *root bud*.

In figures, the root bud is represented by a double red arrow, see for instance Figure 6(A).

In genus 0, this convention implies that rooted unicellular blossoming maps are blossoming plane trees with a marked bud. It corresponds to *planted plane trees* as considered originally in [17].

3.2. Closure of blossoming maps. The closure of a blossoming map consists in matching its buds and leaves in a canonical way. Informally, buds and leaves are respectively seen as opening

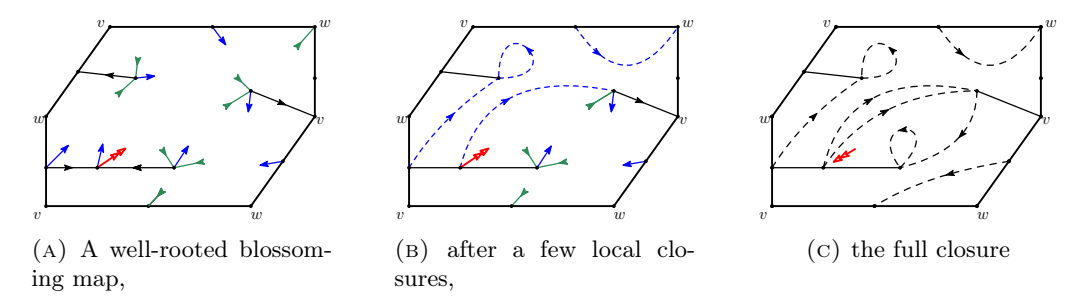


FIGURE 6. The closure of a well-rooted blossoming map.

and closing parentheses and are matched as in a parenthesis word. We give in this section two (more formal) equivalent definitions of the closure operation.

3.2.1. First definition of closure. Let $\mathfrak u$ be a rooted blossoming unicellular map, with the same number of leaves and buds. The closure of $\mathfrak u$ is defined as follows (see Figure 6). The clockwise contour of $\mathfrak u$ induces a cyclic ordering, denoted \preceq , on the stems. Let β be a bud (incident to $v \in V(\mathfrak u)$) such that the next stem for \preceq after β is a leaf ℓ (incident to $w \in V(\mathfrak u)$). The local closure of β consists in merging β and ℓ into an edge $\{v,w\}$ oriented from v to w. The local closure produces a new face which lies on the left of $\{v,w\}$ and which is denoted $f(\ell)$.

Next the *closure* of $\mathfrak u$ is the map obtained by performing iteratively all possible local closures (after each local closure, the ordering on the stems is obtained by removing the two stems involved in the local closure from the previous ordering). The resulting map is rooted on the corner preceding the root bud before its closure.

We can prove that the closure is well-defined in the sense that it does not depend on the order in which the local closures are performed, and that there are no remaining unmatched stems in the closure.

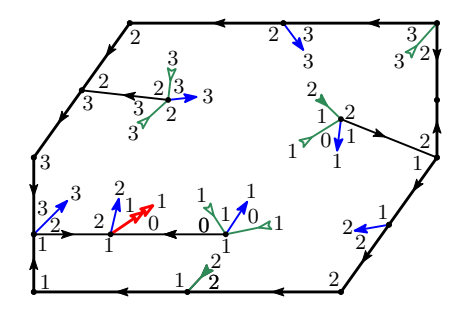
Definition 3.1. A rooted blossoming unicellular map $\mathfrak u$ with the same number of leaves and buds is called well-rooted if the local closure involving its root bud can be the last local closure performed³ Equivalently, a rooted blossoming map is well-rooted, if there is no local closure involving a bud β and a leaf ℓ such that $\beta \leq \rho \leq \ell$.

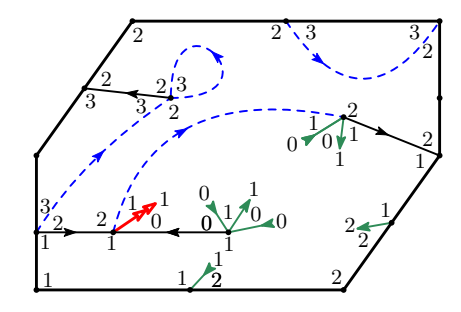
Equivalently, flip the orientation of the root bud of $\mathfrak u$ to transform it into a "root leaf" and perform all the possible local closures. The resulting map will have two unmatched leaves and if one of those is the root leaf, then $\mathfrak u$ is well-rooted.

Let \mathfrak{u} be a blossoming map and denote by $\chi(\mathfrak{u})$ its closure. There is a clear bijection between edges of $\chi(\mathfrak{u})$ and the reunion of $E(\mathfrak{u})$ and of the set of leaves of \mathfrak{u} . The edges in the image of $E(\mathfrak{u})$ in $\chi(\mathfrak{u})$ are called *proper edges* and the other edges of $\chi(\mathfrak{u})$ are called *closure edges*. In the following, we identify $E(\mathfrak{u})$ and the set of *proper-edges* of $\chi(\mathfrak{u})$ and view \mathfrak{u} as a submap of $\chi(\mathfrak{u})$.

- 3.2.2. Closure with labels. We now present an alternative description of the closure, slightly more formal, which is built upon a labeling of the corners. Let \mathfrak{u} be a rooted blossoming unicellular map. Recall that $C(\mathfrak{u})$ denotes the set of its corners. We define the canonical labeling $\lambda: C(\mathfrak{u}) \to \mathbb{Z}$ of \mathfrak{u} as follows. First, $\lambda(\rho_{\mathfrak{u}}) = 0$. Then, we perform a clockwise contour of \mathfrak{u} and apply the following rules. Let κ_1 and κ_2 be two successive corners, then the label $\lambda(\kappa_2)$ of κ_2 is equal to:
 - $\lambda(\kappa_1)$ if κ_1 and κ_2 are incident along a common edge,
 - $\lambda(\kappa_1) + 1$ if κ_1 and κ_2 are separated by a bud,
 - $\lambda(\kappa_1) 1$ if κ_1 and κ_2 are separated by a leaf.

³In Schaeffer's original paper [17], well-rooted unicellular maps of genus 0 are called *balanced trees*. But, in some recent works, see for instance [15], the authors called *balanced orientations*, some orientations which satisfy a property analogue to the one defining bicolorable orientations. To avoid confusion, we hence stick to the terminology "well-rooted" as introduced in [14]





- (A) A blossoming map endowed with its canonical labeling,
- (B) and after a few partial closures.

FIGURE 7. Illustration of local closures based on labels. The 4-valent unicellular blossoming map $\mathfrak u$ represented in (A) is well-rooted, well-oriented and well-labeled: it is a good map.

The canonical labeling can be extended from corners to stems: for a stem σ adjacent to 2 corners with labels i and i+1, we set $\lambda(\sigma)=i+1$, see Figure 7(A).

We can now give an equivalent definition of the closure procedure. Consider $\mathfrak u$ endowed with its canonical labeling. For any bud β , denote $\ell_{\mathfrak u}(\beta)$ the first leaf after β (for \preceq) such that $\lambda(\beta) = \lambda(\ell_{\mathfrak u}(\beta))$. Then the *closure based on labels* of $\mathfrak u$ is the map obtained by merging β and $\ell_{\mathfrak u}(\beta)$ into an oriented edge. The resulting map is rooted on the corner preceding the root bud before the closure.

The following result follows straightforwardly from the definitions:

Proposition 3.2. Let $\mathfrak u$ be a rooted unicellular blossoming map, with the same number of leaves and buds. Then the closure of $\mathfrak u$ and the closure based on labels of $\mathfrak u$ coincide.

Moreover, u is well-rooted if and only if all its labels are non-negative.

3.2.3. Closure and orientations. For $\mathfrak u$ a unicellular blossoming map with the same number of leaves and buds, observe that the closure edges of $\chi(\mathfrak u)$ are naturally oriented. To endow $\chi(\mathfrak u)$ with an orientation, it is therefore only necessary to prescribe the orientation of its proper edges. In other words, it is enough to orient the edges of $\mathring{\mathfrak u}$.

In the following, we endow rooted unicellular maps in the following canonical way. We perform a clockwise contour of their unique face, and orient each proper edge backwards the first time it is followed. (Since the surfaces we consider are orientable, the orientation will be forward the second time the edge is followed.) This yields the following definition.

Definition 3.3 (well-oriented map). A blossoming unicellular map is called well-oriented if it is endowed with the latter orientation.

3.3. Good blossoming maps and closures. The closure operation defined in the previous section can be applied *a priori* to any family of blossoming maps. Nevertheless, to obtain some interesting results, we now apply the closure to a specific family of maps. We follow the presentation of [14, Section 3]. In this section, we always assume that unicellular maps are canonically well-oriented.

We first extend the labeling of corners to non-necessarily unicellular maps, in the following way:

Definition 3.4 (well-labeled map). A blossoming oriented map is said to be well-labeled if its corners are labeled in such a way that:

- the root corner is labeled 0.
- the labels of two corners lying on the same side of an edge coincide, and
- the labels of two corners adjacent around a vertex differ by 1, in which case the higher label sits on the left of the separating edge (or stem).

If such a labeling exists, it is called a good labeling of \mathfrak{m} .

Note first that an oriented map admits at most one good labeling. If \mathfrak{u} is a rooted unicellular well-oriented blossoming map, \mathfrak{u} is well-labeled if and only if the labeling λ of its corners defined in Section 3.2.2 is a good labeling.

Claim 3.5. Let m be an oriented map, then m admits a good labeling if and only if its underlying orientation is bicolorable.

Consequently, the closure of a rooted well-oriented and well-labeled unicellular map is a bicolorable map endowed with its dual-geodesic orientation.

Proof. Let \mathfrak{m} be a (possibly blossoming) map endowed with a good labeling of its corners. Then, from the sequence of labels of corners around any fixed vertex, it is clear that the orientation is Eulerian.

Assume now that \mathfrak{m} has no stem. It follows from the definition of a good labeling that all the corners incident to the same face has the same label, and define the label of the face to be this common value. Consider an oriented loop ℓ drawn on the underlying surface. Then, in the sequence of labels of faces visited by ℓ , the label increases by one if and only if the edge crosses ℓ from left to right and decreases by one otherwise. It implies that the orientation of \mathfrak{m} is bicolorable.

The closure of a well-labeled unicellular map is naturally endowed with a (good) labeling of its corners, hence the closure is bicolorable. Moreover if the unicellular map is well-oriented, then no clockwise cycle can be created during the closure so that it concludes the proof by Theorem 2.3.

In the rest of this section, we will state that the closure operation can be reversed and that, reciprocally, to a bicolorable map corresponds a unique well-labeled well-oriented unicellular blossoming map.

Definition 3.6. The set of well-rooted, well-labeled, well-oriented unicellular blossoming maps of genus g is denoted by \mathcal{O}_g^{\times} .

Moreover, the subset of \mathcal{O}_g^{\times} restricted to 4-valent maps is denoted \mathcal{O}_g^{\times} and the elements of \mathcal{O}_g^{\times} are called good maps.

Let $\mathfrak{o} \in \mathcal{O}_g$. A leaf ℓ of \mathfrak{o} is said to be *black* (respectively *white*) if $\lambda(\ell)$ is *even* (respectively *odd*). The set of black and white leaves of \mathfrak{o} are respectively denoted $\ell_{\bullet}(\mathfrak{o})$ and $\ell_{\circ}(\mathfrak{o})$. We then define the corresponding generating series as:

$$O_g(z_{\bullet}, z_{\circ}; d_1, d_2, \dots; t) = \sum_{\mathfrak{o} \in \mathcal{O}_g} t^{|E(\hat{\mathfrak{o}})|} z_{\bullet}^{|\ell_{\bullet}(\mathfrak{o})|+1} z_{\circ}^{|\ell_{\circ}(\mathfrak{o})|} \prod_{i > 1} d_i^{n_i(\mathfrak{o})},$$

where, for each $i \geq 1$, $n_i(\mathfrak{m})$ denotes the number of vertices of degree 2i of \mathfrak{o} . And similarly, we define:

$$O_g^{\times}(z_{\bullet},z_{\circ}) = \sum_{\mathfrak{o} \in \mathcal{O}_{\alpha}^{\times}} z_{\bullet}^{|\ell_{\bullet}(\mathfrak{o})|+1} z_{\circ}^{|\ell_{\circ}(\mathfrak{o})|}.$$

Remark 3.1. The asymmetry in z_{\bullet} and z_{\circ} in the definition of O_g comes from the asymmetry in the rooting convention of blossoming maps (and more precisely from the fact that the root bud is always matched with a white leaf). A simple way to remember this convention – which will be useful in the sequel – is to think of the root bud as a black leaf. So that an element of \mathcal{O}_g which contributes with a weight $z_{\bullet}^{\bullet \bullet} z_{\circ}^{n \bullet}$ to O_g has n_{\bullet} black leaves (including the root bud).

We can now state the following theorem, which refines [14, Theorem 3.14]:

Theorem 3.7. The closure operation is a bijection between \mathcal{O}_g and \mathcal{BC}_g , preserving the degree distribution of the vertices. Therefore, its restriction to 4-valent maps yields a bijection between \mathcal{O}_g^{\times} and \mathcal{BC}_g^{\times} .

 \mathcal{O}_g^{\times} and \mathcal{BC}_g^{\times} .

Moreover for $\mathfrak{o} \in \mathcal{O}_g$, it induces a bijection between $\ell_{\circ}(\mathfrak{o})$ and $F_{\circ}(\chi(\mathfrak{o}))$ on one hand and between $\ell_{\bullet}(\mathfrak{o})$ and $F_{\bullet}(\chi(\mathfrak{o}))\setminus\{f_{\rho}\}$ on the other hand. Hence we have the following equality of generating series:

$$O_q(z_{\bullet}, z_{\circ}; d_1, d_2, \dots; t) = BC_q(z_{\bullet}, z_{\circ}; d_1, d_2, \dots; t)$$
 and $O_q^{\times}(z_{\bullet}, z_{\circ}) = BC_q^{\times}(z_{\bullet}, z_{\circ}).$

Proof. Theorem 3.14 of [14] states that the closure operation is a bijection between \mathcal{O}_g and \mathcal{BC}_g , such that the number of leaves of a map in \mathcal{O}_g is equal to the number of non-root faces of its closure.

Let $\mathfrak{o} \in \mathcal{O}_g$ and let $\mathfrak{m} = \chi(\mathfrak{o})$. The definition of the closure based on labels ensures that all the corners incident to the same face f of $\Phi(\mathfrak{o})$ have the same label, that we call height of f, and denote by h(f). Moreover, recall that for any leaf ℓ of \mathfrak{m} , $f(\ell)$ is the face of $\Phi(\mathfrak{o})$ situated on the left of the closure edge associated to ℓ . Therefore f is a bijection between the set of leaves of \mathfrak{m} and $\mathcal{F}_{\Phi(\mathfrak{o})} \setminus f_{\rho}$, such that, additionally, the label of ℓ and $f(\ell)$ coincide. Consequently, since \mathfrak{m} is bicolorable, f is a bijection between black (resp. white) leaves of o and black (resp. white) non-root faces of \mathfrak{m} . Since the root face of \mathfrak{m} is black by definition, this concludes the proof. \square

Combining Theorem 3.7 and Proposition 2.1 gives the following result:

Corollary 3.8. The closure operation combined with the radial construction gives a bijection between \mathcal{O}_g^{\times} and \mathcal{M}_g . And, for any $g \geq 0$, we furthermore have the following equality of generating series:

$$M_q(z_{\bullet}, z_{\circ}) = O_q^{\times}(z_{\bullet}, z_{\circ}).$$

Remark 3.2. In view of the preceding corollary, to give a combinatorial proof of Theorem 1.2, it is enough to prove that a similar result holds with O_g^{\times} in lieu of M_g . That is why, from now on and until the end of the article, we only deal with 4-valent maps and in particular with good maps.

3.4. Analysis of good maps. The now typical approach developed in [8] to enumerate unicellular maps consists in decomposing a map into a core (as defined in Section 2.4) on which are grafted some trees. However, some technical issues need to be taken care of before applying this general strategy. The first issues already appeared in [14] and can be treated in the same way by using some "rerooting" techniques.

A new complication appears, due to the fact that the distribution of white and black leaves is not stable via the rerooting operation. However, we prove in Theorem 3.11 that its effect averages on some subsets of maps, which is enough for our purposes.

3.4.1. Rootable stems and unrooted maps. We start with some definitions.

Definition 3.9 (rootable stem, well-rootable stem). A stem is called rootable if it is either a leaf or the root bud. The set of rootable stems of a map \mathfrak{m} is denoted $S^{\rho}(m)$.

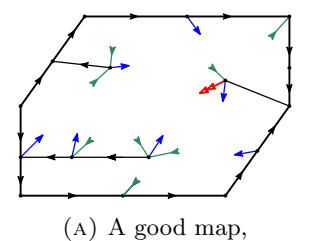
Definition 3.10 (unrooted map). Two rooted blossoming unicellular maps are called root-equivalent if they have the same interior map and the same set of stems and of rootable stems (in particular, they do not necessarily have the same root). In other words, $\mathfrak u$ and $\mathfrak u'$ are root-equivalent if there exists $\sigma \in S^{\rho}(\mathfrak u)$, such that $\mathfrak u'$ can be obtained from $\mathfrak u$ by turning the root bud of $\mathfrak u$ into a leaf and transforming σ into the root bud of $\mathfrak u'$.

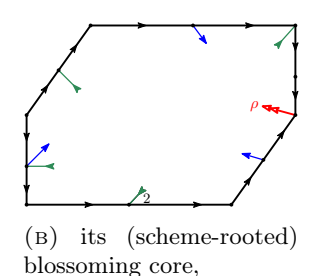
The unrooted map of a rooted unicellular blossoming map $\mathfrak u$ is the equivalence class of $\mathfrak u$ for root-equivalence.

3.4.2. Blossoming cores and schemes. The definitions of schemes and cores given in Section 2.4 for unicellular maps can be extended to unicellular blossoming maps. Blossoming cores and blossoming schemes are then defined as unicellular blossoming maps with only vertices of interior degree greater than 1 and 2 respectively.

However, special care needs to be taken to handle leaves and buds when computing the core and the scheme of a unicellular blossoming map. Let $\mathfrak u$ be a unicellular blossoming map. To construct its blossoming core $\Psi(\mathfrak u)$, we procede as follows. For any $v \in \mathfrak u$ of interior degree one, let w be the unique vertex incident to v. Erase v together with its stems, and add a stem σ adjacent to w in place of the former edge $\{v, w\}$, , see Figure 8.

In a blossoming core, vertices of interior degree 3 are called *scheme vertices* and subsequently stems incident to scheme-vertices are called *scheme-stems*. If its root bud is a scheme-stem, a blossoming core is said to be *scheme-rooted*.





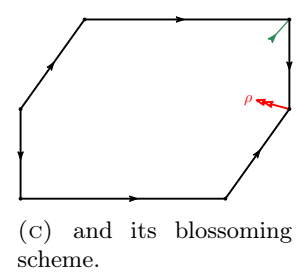


FIGURE 8. The blossoming core and scheme of a blossoming well-oriented scheme-rooted unicellular map.

The scheme $\Theta(\mathfrak{c})$ of a scheme-rooted blossoming core \mathfrak{c} is the map obtained from \mathfrak{c} by removing its vertices of interior degree 2, together with their incident stems. Vertices of interior degree 2 in \mathfrak{c} form sequences called *branches* between its scheme vertices, so that each branch of \mathfrak{c} is replaced by an edge in $\Theta(\mathfrak{c})$. Moreover, we identify scheme-vertices and scheme-stems of \mathfrak{c} with their image in $\Theta(\mathfrak{c})$.

Note that if a unicellular map is endowed with an orientation then its core inherits its orientation. In particular, it is easy to see that the blossoming core of a well-oriented unicellular map is also canonically well-oriented, as illustrated on Figure 8(B). Moreover, if \mathfrak{c} is a well-oriented scheme-rooted blossoming core, the orientation of all edges inside one its branches coincide, so that $\Theta(c)$ is also naturally endowed with an orientation. Again, it is easy to see that $\Theta(c)$ is well-oriented, see Figure 8(C).

In the rest of the paper, all the families of unicellular maps (or families in bijection with some sets of unicellular maps by Theorem 3.7) can be refined by specifying the unrooted scheme (or the unrooted scheme of their image by the bijection). For instance, we denote $\mathcal{BC}_{\bar{s}}^{\times}$, the subset of \mathcal{BC}^{\times} such that $\mathfrak{m} \in \mathcal{BC}_{\bar{s}}^{\times}$ if and only if the unrooted scheme of $\chi^{-1}(\mathfrak{m})$ is equal to \bar{s} .

3.4.3. Main result. The set of scheme-rooted well-labeled well-oriented 4-valent blossoming cores is denoted \mathcal{R} . The subset of \mathcal{R} restricted to cores of genus g with $n_{\bullet}-1$ black leaves and n_{\circ} white leaves is denoted $\mathcal{R}_{g;n_{\bullet},n_{\circ}}$, and the generating series $R^{\times}(z_{\bullet},z_{\circ})$ is hence defined as:

$$R^{\times}(z_{\bullet}, z_{\circ}) = \sum_{n_{\bullet} \geq 0, n_{\circ} \geq 0} |\mathcal{R}_{g; n_{\bullet}, n_{\circ}}| z_{\bullet}^{n_{\bullet}} z_{\circ}^{n_{\circ}}.$$

We can now state the main result of this section:

Theorem 3.11. Let $\mathfrak{r} \in \mathcal{R}$. Then, the following equality of generating series holds:

$$O_{\overline{\mathfrak{r}}}^{\times}(z_{\bullet},z_{\circ}) = \frac{R_{\overline{\mathfrak{r}}}(T_{\bullet},T_{\circ}) + R_{\overline{\mathfrak{r}}}(T_{\circ},T_{\bullet})}{2g - |\mathring{n}_{2}(\overline{\mathfrak{r}})|},$$

where $\mathring{n}_2(\overline{r})$ denotes the set of vertices of interior degree 4 in $\overline{\mathfrak{r}}$ and T_{\bullet} and T_{\circ} are the generating series defined in (1) of Theorem 1.2.

This result is a generalization of [14, Lemma 4.12]. It requires two rerooting steps coupled with a pruning procedure, along with an analysis of the evolution of the parity of labels during the rerooting. Its proof requires to introduce a couple of additional definitions and is the purpose of the next section.

3.5. Proof of Theorem 3.11.

3.5.1. Combinatorial interpretation of T_{\bullet} and T_{\circ} . As mentioned above, when constructing the core of a unicellular blossoming map, the deleted edges form a forest of rooted blossoming plane trees. We now characterize these trees.

Let \mathcal{T}^{\times} be the set of well-oriented, well-labeled, 4-valent unicellular rooted maps of genus 0. We adopt the convention that the map reduced to a single leaf with no vertex belongs to \mathcal{T}^{\times} . Elements of \mathcal{T}^{\times} can alternatively be characterized as follows. They are 4-valent blossoming plane trees with

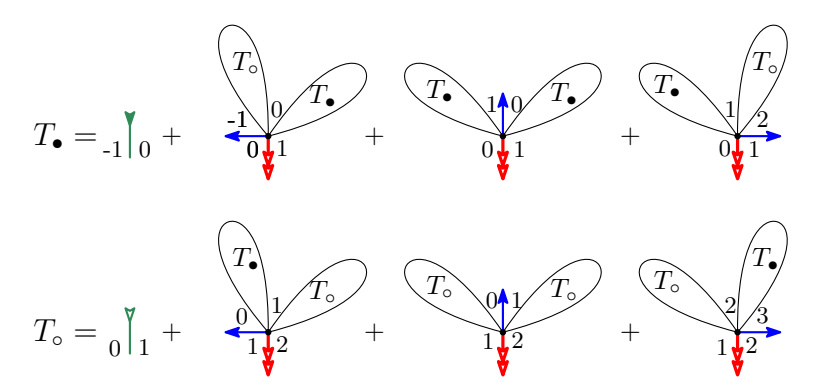


FIGURE 9. Schematic representation of the decomposition of trees in \mathcal{T}^{\times} that translate into the relations (2) for generating series. Labels around the root vertex are indicated.

a marked bud, in which all the interior edges are oriented from a vertex to its parent. Moreover, the fact that they are well-labeled implies that each interior vertex of $\mathfrak{t} \in \mathcal{T}^{\times}$ is incident to exactly one bud, except for the root vertex which is incident to two buds. With this reformulation, it is clear that \mathcal{T}^{\times} corresponds exactly to the family of trees originally introduced by Schaeffer in [17].

Next, recall that in a well-labeled blossoming map, leaves are incident to two corners which are labeled i and i-1 in counterclockwise order around its incident vertex. If i is even (respectively odd), the corresponding leaf is called a *black leaf* (respectively a *white leaf*). In the sequel, it will be useful to introduce the two following bivariate generating series T_{\bullet} and T_{\circ} to enumerate elements of \mathcal{T}^{\times} :

$$(2) \ T_{\bullet}(z_{\bullet}, z_{\circ}) = z_{\bullet} + \sum_{\substack{t \in \mathcal{T}^{\times} \\ t \text{ not empty}}} z_{\bullet}^{|\ell_{\bullet}(\mathfrak{t})|} z_{\circ}^{|\ell_{\circ}(\mathfrak{t})|} \qquad \text{and} \qquad T_{\circ}(z_{\bullet}, z_{\circ}) = z_{\circ} + \sum_{\substack{t \in \mathcal{T}^{\times} \\ t \text{ not empty}}} z_{\bullet}^{|\ell_{\circ}(\mathfrak{t})|} z_{\circ}^{|\ell_{\bullet}(\mathfrak{t})|}.$$

Alternatively T_{\circ} can be defined as the generating series of elements of \mathcal{T}^{\times} , in which all the labels are shifted by 1, so that white leaves become black leaves and vice-versa. With this presentation in mind, standard decomposition of trees as illustrated in Figure 9 allows to retrieve the following equations already given in (1):

$$\begin{cases} T_{\bullet} = z_{\bullet} + T_{\bullet}^{2} + 2T_{\circ}T_{\bullet} \\ T_{\circ} = z_{\circ} + T_{\circ}^{2} + 2T_{\circ}T_{\bullet}. \end{cases}$$

These equations uniquely characterize T_{\bullet} and T_{\circ} as formal power series in two variables without constant term. Hence, this gives a combinatorial interpretation of the series involved in the rational parametrization of Theorem 1.2.

3.5.2. Scheme trunks and rerooting.

Definition 3.12. Let \mathfrak{o} be a good blossoming unicellular map. A scheme trunk of \mathfrak{o} is either:

- an edge incident to a scheme vertex, which does not belong to the core (i.e, it is the "trunk" of a tree attached to the scheme),
- or, a rootable stem incident to a scheme vertex.

Definition 3.13. Let $\mathfrak{r} \in \mathcal{R}$. A 4-valent scheme-rooted tree-decorated core is defined as $\mathfrak{r}^* = (\mathfrak{r}, (\mathfrak{t}_{\sigma})_{\sigma \in S^{\rho}(\mathfrak{r})})$, where (\mathfrak{t}_{σ}) is a collection of trees in \mathcal{T}^{\times} indexed by the rootable stems of \mathfrak{r} . We denote by \mathcal{D} the set of 4-valent scheme-rooted tree-decorated cores.

Let $\mathfrak{s}^* = (\mathfrak{s}, (\mathfrak{t}_{\ell})) \in \mathcal{D}$. A unicellular non-rooted blossoming map with a marked scheme trunk is canonically associated to \mathfrak{s}^* by the following construction, see Figure 10. For any leaf σ of \mathfrak{s} , if \mathfrak{t}_{σ} is empty, do nothing; otherwise graft \mathfrak{t}_{σ} to \mathfrak{s} by merging the root bud of \mathfrak{t}_{σ} with σ . Let ρ be the root

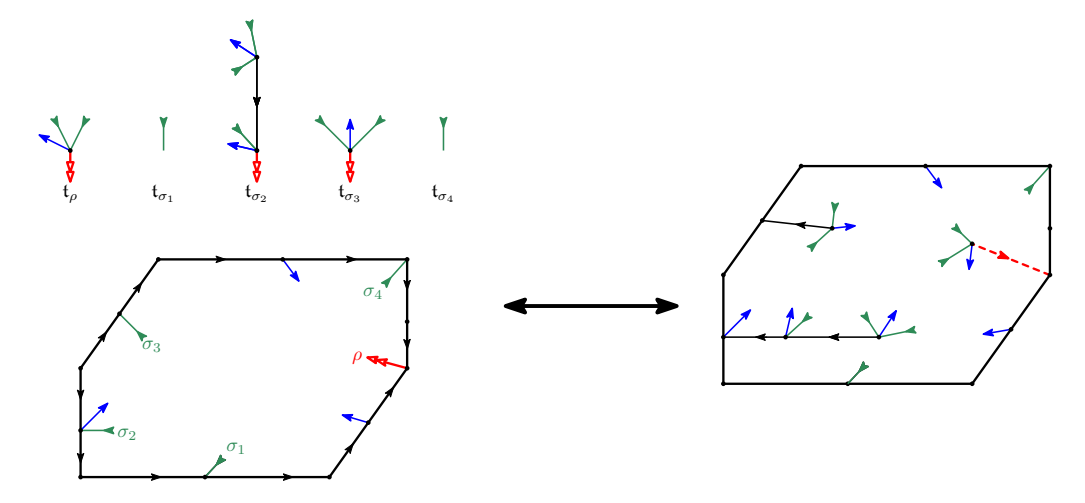


FIGURE 10. The correspondence between a scheme-rooted decorated core (left) and a non-rooted blossoming map with a marked scheme trunk (right)

bud of \mathfrak{s} , graft \mathfrak{t}_{ρ} to \mathfrak{s} by either merging its root bud with ρ and marking the edge thus created if \mathfrak{t}_{ρ} is not empty or by only marking ρ otherwise. In the following, we *identify scheme-rooted tree-decorated cores with the corresponding blossoming maps with a marked scheme trunk*.

Fix $\mathfrak{o} \in \mathcal{O}^{\times}$ and τ a scheme-trunk of \mathfrak{o} . Then, define \mathfrak{o}^{τ} to be the scheme-rooted tree-decorated core obtained by replacing the root bud of \mathfrak{o} by a leaf and by marking τ , see Figures 11(A) and 11(B).

Proposition 3.14. Let $\mathfrak{o} \in \mathcal{O}^{\times}$ and let τ be a scheme trunk of \mathfrak{o} . Then the application which maps (\mathfrak{o}, τ) to \mathfrak{o}^{τ} is a 2-to-1 application between good maps with a marked scheme trunk and \mathcal{D} . Moreover, if we call $\tilde{\mathfrak{o}}$, the other preimage of \mathfrak{o}^{τ} , then:

$$|\ell^{\circ}(\mathfrak{o})| = |\ell^{\bullet}(\tilde{\mathfrak{o}})| + 1, \quad \text{ and } \quad |\ell^{\circ}(\tilde{\mathfrak{o}})| = |\ell^{\bullet}(\mathfrak{o})| + 1.$$

Proof. We first prove that \mathfrak{o}^{τ} belongs to \mathcal{D} , which amounts to showing that $\Psi(\mathfrak{o}^{\tau})$ – the scheme of \mathfrak{o}^{τ} – belongs to \mathcal{R} . First, it is easy to see that the blossoming core of a good map is itself well-labeled and well-oriented (when considering the restriction of the orientation of the original map to the edges that belong to the core). Therefore $\mathfrak{c} := \Psi(\mathfrak{o})$ is a well-labeled well-oriented 4-valent unicellular blossoming map (but it is not scheme-rooted).

By a slight abuse of notation, we denote by τ the rootable stem of \mathfrak{c} which corresponds to τ , see Figure 11(C). Then, define \mathfrak{c}^{τ} to be the map obtained from \mathfrak{c} by changing the root bud into a leaf and changing τ into the root bud, in other words we "reroot" \mathfrak{c} at τ , see Figure 11(D). The proof of [14, Lemma 4.2] can be applied verbatim to prove that \mathfrak{c}^{τ} is still well-labeled and well-oriented, hence it belongs to \mathcal{R} .

Now, let ℓ be the leaf which is matched to the root bud of \mathfrak{o} in its closure. Reroot \mathfrak{o} at ℓ (i.e. transform its root bud into a leaf and turn ℓ into the new root bud), and call $\tilde{\mathfrak{o}}$ the resulting map. Again [14, Lemma 4.2] directly implies that $\tilde{\mathfrak{o}}$ is still a good map, and clearly $(\tilde{\mathfrak{o}})^{\tau} = \mathfrak{o}^{\tau}$. Note that there might exist some non-trivial automorphisms and that \mathfrak{o} and $\tilde{\mathfrak{o}}$ could be equal, but as maps with a marked scheme trunk (\mathfrak{o}, τ) and $(\tilde{\mathfrak{o}}, \tau)$ are necessarily different. So that $(\tilde{\mathfrak{o}}, \tau)$ is another preimage of \mathfrak{o}^{τ} .

To prove that there exists no other preimage of \mathfrak{o}^{τ} in \mathcal{O}^{\times} , it suffices to notice that any other preimage is necessarily root-equivalent to \mathfrak{o} and that at most two different well-rooted maps can admit the same unrooted map.

To finish the proof, observe that, generally, if we pick a rootable stem of \mathfrak{o} and reroot \mathfrak{o} at this stem, then in the new map, either all labels switch parity or none do. Moreover, they switch parity if and only if the picked rootable stem is preceded by a corner with an odd label in \mathfrak{o} . It implies that all labels in \mathfrak{o}^{τ} have different parity than in \mathfrak{o} , see also Figure 11(E). By seeing momentarily

the root bud as a black leaf (as was done in Remark 3.1), it yields a bijection between black leaves of $\tilde{\mathfrak{o}}$ and white leaves of $\tilde{\mathfrak{o}}$ and vice-versa, which concludes the proof.

Proof of Theorem 3.11. Let $\mathfrak{o} \in \mathcal{O}_{\bar{\mathfrak{r}}}^{\times}$. It follows directly from the definition of pruning, that the number of scheme trunks of \mathfrak{o} is equal to the number of rootable scheme-stems of its core. By [14, Lemma 4.7], a blossoming core \mathfrak{c} has $2g - |\mathring{n}_2(\mathfrak{c})|$ rootable scheme-stems (where g denotes the genus of the underlying surface). Hence, \mathfrak{o} has $2g - |\mathring{n}_2(\Psi(\mathfrak{o}))| = 2g - |\mathring{n}_2(\bar{\mathfrak{r}})|$ scheme trunks and $(2g - |\mathring{n}_2(\bar{\mathfrak{r}})|)O_{\bar{\mathfrak{r}}}^{\times}(z_{\bullet}, z_{\circ})$ is the generating series of elements of $\mathcal{O}_{\bar{\mathfrak{r}}}^{\times}$ with a marked scheme trunk.

Then the result relies mostly on Proposition 3.14 and on the classical relation between decomposition of combinatorial classes and composition of generating functions. However, some subtleties appear.

First, observe that, in the pruning operation, if a dangling tree not containing the root bud is replaced by a leaf, then the labels of the corners incident to that leaf are equal to the corresponding corners before deleting the tree. It implies that the labeling of the corners of $\Psi(\mathfrak{o})$ have all either the same parity as the corresponding corners in \mathfrak{o} or the opposite parity.

Fix τ a scheme-trunk of \mathfrak{o} , and consider $\mathfrak{r}^* = (\mathfrak{r}, (\mathfrak{t}_{\sigma})_{\sigma \in S^{\rho}(\mathfrak{r})})$ the scheme-decorated core associated to \mathfrak{o} by Proposition 3.14. Then \mathfrak{r} and $\Psi(\mathfrak{o})$ are root-equivalent and again either their corners have all the same parity or have all opposite parity. Therefore, when substituting the rootable stems of \mathfrak{r} by the trees of the family (\mathfrak{t}_{σ}) , we either have:

(3)
$$|\ell^{\circ}(\mathfrak{o})| = |\ell^{\circ}(\mathfrak{t}_{\rho_{\mathfrak{r}}})| + \sum_{\sigma \in \ell^{\bullet}(\mathfrak{r})} |\ell^{\circ}(\mathfrak{t}_{\sigma})| + \sum_{\sigma \in \ell^{\circ}(\mathfrak{r})} |\ell^{\bullet}(\mathfrak{t}_{\sigma})|$$

or

$$(4) |\ell^{\circ}(\mathfrak{o})| = |\ell^{\bullet}(\mathfrak{t}_{\rho_{\mathfrak{r}}})| + \sum_{\sigma \in \ell^{\bullet}(\mathfrak{r})} |\ell^{\bullet}(\mathfrak{t}_{\sigma})| + \sum_{\sigma \in \ell^{\circ}(\mathfrak{r})} |\ell^{\circ}(\mathfrak{t}_{\sigma})|.$$

Similar equalities hold for the number of black leaves of \mathfrak{o} , but another subtlety appears. Indeed, when replacing leaves of \mathfrak{r} by trees, the root bud of \mathfrak{o} corresponds in fact to a leaf of one of these trees. More precisely, suppose that (3) holds, then we have (and a similar equality if (4) holds):

$$|\ell^{\bullet}(\mathfrak{o})| + 1 = |\ell^{\bullet}(\mathfrak{t}_{\rho_{\mathfrak{r}}})| + \sum_{\sigma \in \ell^{\bullet}(\mathfrak{r})} |\ell^{\bullet}(\mathfrak{t}_{\sigma})| + \sum_{\sigma \in \ell^{\circ}(\mathfrak{r})} |\ell^{\circ}(\mathfrak{t}_{\sigma})|.$$

It concludes the proof, in view of the definition of the generating series O^{\times} and R^{\times} and of the last assertion of Proposition 3.14.

4. Criterion for rationality via Motzkin walks

In this section, we extend the criterion for rationality obtained in [8] to the bivariate case. We first introduce in Section 4.1 a family of weighted paths that will appear naturally in the enumeration of blossoming cores. In Section 4.2, we give a criterion for rationality based on these paths. Finally, in Section 5.1, we give the link between the generating series of blossoming cores and of these paths.

4.1. Weighted Motzkin paths. A Motzkin walk w of length ℓ starting at height h is a walk in $\mathbb{Z}^+ \times \mathbb{Z}$ starting at (0,h) made of ℓ steps w_1, \ldots, w_ℓ , such that $w_i \in \{(1,-1),(1,0),(1,1)\}$, for $1 \leq i \leq \ell$. The set of Motzkin walks is denoted by \mathcal{W} . A step w_i is called horizontal, up or down if its second coordinate is respectively equal to 0, +1 or -1. For $1 \leq k \leq \ell$, the height at time k is equal to the ordinate of the walk when its abscissa is equal to k and the height of the k-th step is the height at time ℓ and the height at time ℓ . The increment of w is the difference between the height at time ℓ and the height at time ℓ .

A *Motzkin bridge* is a Motzkin walk starting at height 0 whose increment is equal to 0. More generally, for $i, j \in \mathbb{Z}$, we denote $W^{i \to j}$ the set of Motzkin walks starting at height i, with increment j - i. A *primitive Motzkin walk* is a Motzkin walk starting at height 0 with increment -1 and such that the height of each step is non-negative.

For $w \in \mathcal{W}$, we denote respectively by h(w), o(w) and e(w), its number of horizontal steps, its number of non-horizontal steps with odd height (called odd steps) and its number of non-horizontal

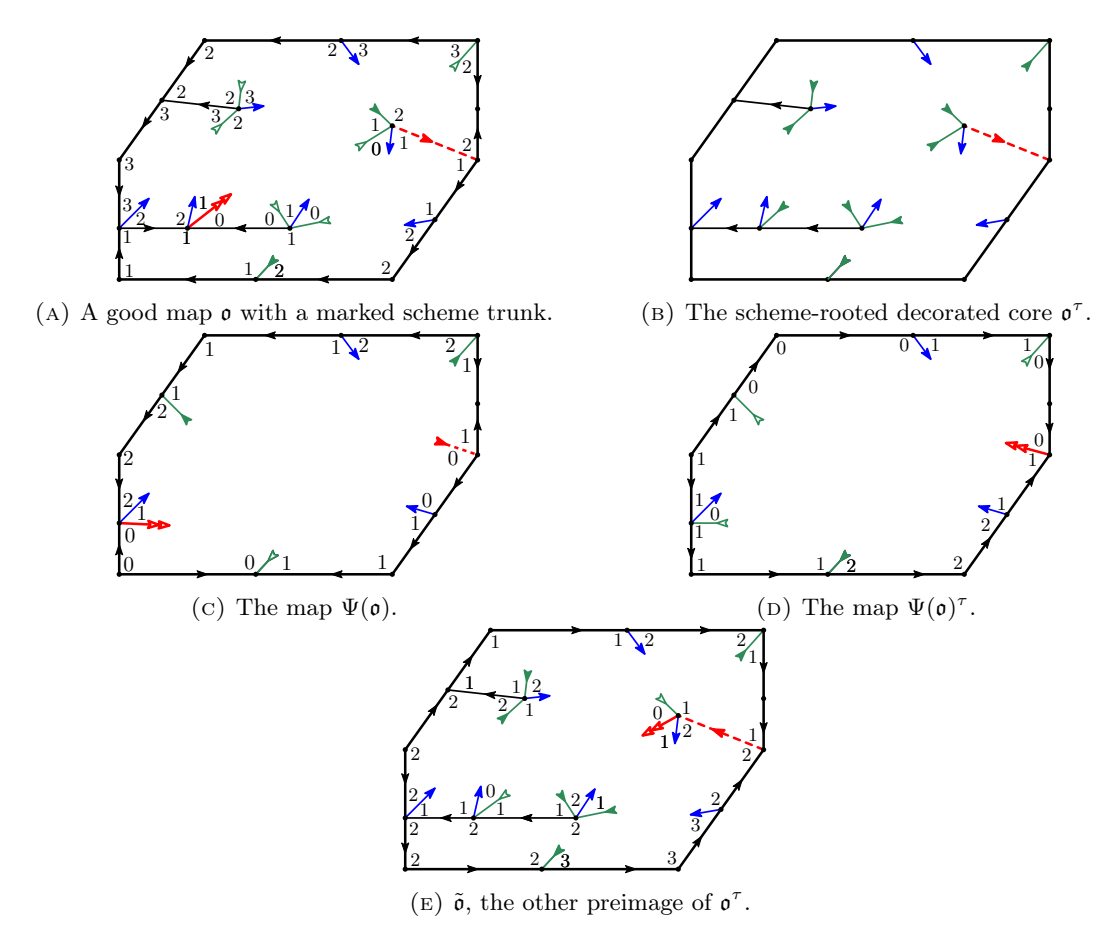


FIGURE 11. The different maps involved in the proof of Theorem 3.11

steps with even height (called even steps). For any $i, j \in \mathbb{Z}$, we introduce the following (weighted) generating series will appear naturally in the next section:

(5)
$$W^{i \to j}(t_{\bullet}, t_{\circ}) = \sum_{\mathbf{w} \in \mathcal{W}^{i \to j}} (2(t_{\bullet} + t_{\circ}))^{h(\mathbf{w})} t_{\bullet}^{e(\mathbf{w})} t_{\circ}^{o(\mathbf{w})}$$

We also consider the following generating series enumerating primitive Motzkin walks and Motzkin bridges:

$$D_{\bullet}(t_{\bullet}, t_{\circ}) = \sum_{\substack{\text{w primitive} \\ \text{Motzkin walks}}} (2(t_{\bullet} + t_{\circ}))^{h(w)} t_{\bullet}^{e(w)} t_{\circ}^{o(w)}$$

$$D_{\circ}(t_{\bullet}, t_{\circ}) = \sum_{\substack{\text{w primitive} \\ \text{Motzkin walks}}} (2(t_{\bullet} + t_{\circ}))^{h(w)} t_{\circ}^{e(w)} t_{\bullet}^{o(w)}$$

$$B(t_{\bullet}, t_{\circ}) = \sum_{\text{w Motzkin bridges}} (2(t_{\bullet} + t_{\circ}))^{h(w)} t_{\bullet}^{e(w)} t_{\circ}^{o(w)}$$

Note, that D_{\circ} could be equivalently defined as the weighted generating series of shifted primitive Motzkin walks, i.e starting at height 1, with increment -1 and staying positive before their last step. More generally, for $k \in \mathbb{Z}$, denote by $W_{[\geq k]}^{k \to (k-1)}(t_{\bullet}, t_{\circ})$ the (weighted) generating series of Motzkin walks, with height not smaller than k, except after their last step. It is immediate to see that

$$W_{[\geq k]}^{k \to (k-1)}(t_{\bullet}, t_{\circ}) = \begin{cases} D_{\bullet} & \text{if } k \text{ is even} \\ D_{\circ} & \text{otherwise.} \end{cases}$$

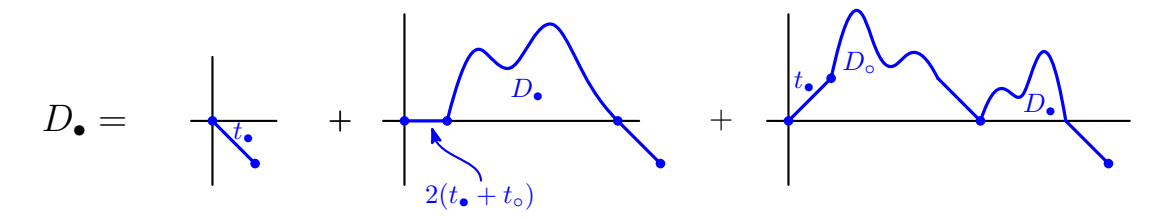


Figure 12. Schematic decomposition of primitive Motzkin walks.

Property 4.1. The generating series D_{\bullet} , D_{\circ} and B satisfy the following "symmetric" relations:

(6)
$$B(t_{\bullet}, t_{\circ}) = B(t_{\circ}, t_{\bullet}) \quad and \quad t_{\circ}D_{\bullet} = t_{\bullet}D_{\circ},$$

and the following decomposition equations:

$$D_{\bullet} = t_{\bullet} + 2(t_{\bullet} + t_{\circ})D_{\bullet} + t_{\bullet} \cdot D_{\circ}D_{\bullet},$$

$$D_{\circ} = t_{\circ} + 2(t_{\bullet} + t_{\circ})D_{\circ} + t_{\circ} \cdot D_{\bullet}D_{\circ},$$

$$B = 1 + 2(t_{\bullet} + t_{\circ})B + (t_{\bullet}D_{\circ} + t_{\circ}D_{\bullet})B.$$

Proof. In a Motzkin bridge, the number of odd up-steps is clearly equal to the number of even down-steps and the number of even up-steps is equal to the number of odd down-steps, so that the number of odd steps is equal to the number of even steps. Therefore, a symmetry around a vertical axis gives the first equality. The same argument applied to positive bridges (enumerated by $\frac{D_{\bullet}}{t_{\bullet}}$) proves the second equality.

It follows directly from (6), that for any $k \in \mathbb{Z}$, $B(t_{\bullet}, t_{\circ}) = W^{k \to k}(t_{\bullet}, t_{\circ})$. Hence, the three decomposition equations are obtained by the first-passage to 0 classical decomposition (see e.g. [12, Section I.5.3), illustrated in Figure 12 in the case of D_{\bullet} . П

4.2. Symmetry and rationality. The relations stated in Property 4.1 imply that t_{\bullet} and t_{\circ} might be viewed as rational functions in D_{\bullet} and D_{\circ} defined as follows:

(7)
$$t_{\bullet}(D_{\bullet}, D_{\circ}) = \frac{1}{D_{\circ} + 2\left(\frac{D_{\circ}}{D_{\bullet}} + 1\right) + \frac{1}{D_{\bullet}}},$$
(8)
$$t_{\circ}(D_{\bullet}, D_{\circ}) = \frac{1}{D_{\bullet} + 2\left(\frac{D_{\bullet}}{D_{\circ}} + 1\right) + \frac{1}{D_{\circ}}}.$$

(8)
$$t_{\circ}(D_{\bullet}, D_{\circ}) = \frac{1}{D_{\bullet} + 2\left(\frac{D_{\bullet}}{D_{\circ}} + 1\right) + \frac{1}{D_{\circ}}}.$$

This expression implies in particular that any function in the two variables t_{\bullet} and t_{\circ} can be seen as a function in D_{\bullet} and D_{\bullet} .

Definition 4.2. Let f(x,y) be a function of two variables, we say that

- $\begin{array}{l} \bullet \ f \ is \ \mathrm{symmetric} \ if \ f(x,y) = f(y,x), \\ \bullet \ f \ is \ \parallel\text{-symmetric} \ if \ f(x,y) = f(x^{-1},y^{-1}). \\ \bullet \ f \ is \ \times\text{-symmetric} \ if \ f(x,y) = f(y^{-1},x^{-1}). \end{array}$

We denote by f^{\bullet} the function defined by $f^{\bullet} = f(x,y) + f(y,x)$, so that f^{\bullet} is always symmetric and is \parallel -symmetric if and only if is \times -symmetric.

We also denote by \overline{f}^{\parallel} the function such that $\overline{f}^{\parallel}(x,y)=f(x^{-1},y^{-1})$, so that f is \parallel -symmetric if and only if $f = \overline{f}^{\parallel}$.

For instance, it is clear from (7) and (8) that – as functions of D_{\bullet} and D_{\circ} – t_{\bullet} and t_{\circ} are \times -symmetric.

Based on these definitions, we get the following nice criterion for rationality in z_0 and z_{\bullet} , extending [8, Lemma 9].

Lemma 4.3. Let f be a symmetric function and write F for the function such that $F(D_{\circ}, D_{\bullet}) = f(t_{\circ}, t_{\bullet})$. Then F is also symmetric.

Moreover, the two following properties are equivalent:

- (i) f is a rational function.
- (ii) F is a rational function and is \parallel -symmetric

Proof. We start by proving that F is symmetric. The definition of D_{\circ} and D_{\bullet} immediately implies that $D_{\circ}(t_{\circ}, t_{\bullet}) = D_{\bullet}(t_{\bullet}, t_{\circ})$. We can then write:

$$F(D_{\circ}, D_{\bullet}) = f(t_{\circ}, t_{\bullet}) = f(t_{\bullet}, t_{\circ}) = F(D_{\bullet}, D_{\circ}),$$

hence F is symmetric. The implication $(i) \implies (ii)$ is clear from the expression of t_{\circ} and t_{\bullet} in terms of D_{\circ} and D_{\bullet} .

We now turn our attention to the implication $(ii) \implies (i)$. Since F is symmetric and \parallel -symmetric, it is also \times -symmetric. Consider the vector space of polynomials in D_{\circ} , D_{\circ}^{-1} , D_{\bullet} , and D_{\bullet}^{-1} , that are symmetric, \parallel -symmetric, and \times -symmetric. The natural basis for this vector space is $(D_{i,j})_{0 \le i \le j} := \left(D_{\circ}^i D_{\bullet}^j + D_{\circ}^j D_{\bullet}^i + D_{\circ}^{-i} D_{\bullet}^{-j} + D_{\circ}^{-j} D_{\bullet}^{-i}\right)_{0 \le i \le j}$.

We prove by induction on i+j that $D_{i,j}$ (with $0 \le i \le j$) can be written down as a polynomial in t_{\bullet}^{-1} and t_{\bullet}^{-1} :

$$t_{\bullet}^{-i}t_{\circ}^{-j} = \left(D_{\circ} + 2\left(\frac{D_{\circ}}{D_{\bullet}} + 1\right) + \frac{1}{D_{\bullet}}\right)^{i} \cdot \left(D_{\bullet} + 2\left(\frac{D_{\bullet}}{D_{\circ}} + 1\right) + \frac{1}{D_{\circ}}\right)^{j}$$

$$= D_{\circ}^{i}\left(1 + 2\left(\frac{1}{D_{\bullet}} + \frac{1}{D_{\circ}}\right) + \frac{1}{D_{\circ}D_{\bullet}}\right)^{i} \cdot D_{\bullet}^{j}\left(1 + 2\left(\frac{1}{D_{\circ}} + \frac{1}{D_{\bullet}}\right) + \frac{1}{D_{\bullet}D_{\circ}}\right)^{j}$$

$$= D_{\circ}^{i}D_{\bullet}^{j}\left(1 + p_{i}\left(\frac{1}{D_{\bullet}}, \frac{1}{D_{\circ}}\right)\right)\left(1 + p_{j}\left(\frac{1}{D_{\bullet}}, \frac{1}{D_{\circ}}\right)\right),$$

where p_i and p_j are polynomials with no constant term.

This implies that any monomial of $t_{\circ}^{-i}t_{\circ}^{-j} - D_{\circ}^{i}D_{\circ}^{j}$ of the form $D_{\circ}^{k}D_{\bullet}^{l}$ with $k,l \geq 0$, satisfies k+l < i+j. Similarly, any monomial of $t_{\circ}^{-i}t_{\circ}^{-j} - D_{\circ}^{-i}D_{\circ}^{-j}$ of the form $D_{\circ}^{-k}D_{\bullet}^{-l}$ with $k,l \geq 0$, satisfies k+l < i+j. By consequence (assuming that $i+j \neq 0$), any monomial of $t_{\circ}^{-i}t_{\circ}^{-j} - D_{\circ}^{i}D_{\bullet}^{-j} - D_{\circ}^{-i}D_{\circ}^{-j}$ of the form $D_{\circ}^{-k}D_{\bullet}^{-l}$ or $D_{\circ}^{k}D_{\bullet}^{l}$ with $k,l \geq 0$, satisfies k+l < i+j. By a \circ/\bullet exchange, we also obtain that any monomial of $t_{\circ}^{-i}t_{\bullet}^{-j} - D_{\bullet}^{i}D_{\circ}^{j} - D_{\circ}^{-i}D_{\bullet}^{-j}$ of the form $D_{\bullet}^{-k}D_{\circ}^{-l}$ or $D_{\bullet}^{k}D_{\circ}^{l}$ with $k,l \geq 0$, satisfies k+l < i+j.

As a function of D_{\circ} and D_{\bullet} , $t_{\bullet}^{-i}t_{\circ}^{-j}+t_{\circ}^{-i}t_{\bullet}^{-j}$ is rational, \parallel -symmetric, and \times -symmetric. Hence so is $t_{\bullet}^{-i}t_{\circ}^{-j}+t_{\circ}^{-i}t_{\bullet}^{-j}-D_{i,j}$, which can therefore be written as a linear combination of $(D_{k,l})_{0\leq k\leq l}$. Since $t_{\bullet}^{-i}t_{\circ}^{-j}+t_{\circ}^{-i}t_{\bullet}^{-j}-D_{i,j}=(t_{\bullet}^{-i}t_{\circ}^{-j}-D_{\circ}^{i}D_{\bullet}^{j}-D_{\bullet}^{-i}D_{\circ}^{-j})+(t_{\circ}^{-i}t_{\bullet}^{-j}-D_{\bullet}^{i}D_{\circ}^{j}-D_{\circ}^{-i}D_{\bullet}^{-j})$, and because of the result of the previous paragraph, the decomposition of $t_{\bullet}^{-i}t_{\circ}^{-j}+t_{\circ}^{-i}t_{\bullet}^{-j}-D_{i,j}$ on the basis $(D_{i,j})_{0\leq i\leq j}$ can not have terms of the form $D_{k,l}$ with $k+l\geq i+j$. The induction hypothesis implies that $t_{\bullet}^{-i}t_{\circ}^{-j}+t_{\circ}^{-i}t_{\bullet}^{-j}-D_{i,j}$ is a polynomial of t_{\circ}^{-1} and t_{\bullet}^{-1} . Therefore, so is $D_{i,j}$.

To conclude the proof, let P and Q be two bivariate polynomials such that F = P/Q. Since F is symmetric and \parallel -symmetric, we clearly have:

$$\begin{split} F(D_{\circ}, D_{\bullet}) &= \frac{1}{4} \left(\frac{P(D_{\circ}, D_{\bullet})}{Q(D_{\circ}, D_{\bullet})} + \frac{P(1/D_{\circ}, 1/D_{\bullet})}{Q(1/D_{\circ}, 1/D_{\bullet})} + \frac{P(1/D_{\bullet}, 1/D_{\circ})}{Q(1/D_{\bullet}, 1/D_{\circ})} + \frac{P(D_{\bullet}, D_{\circ})}{Q(D_{\bullet}, D_{\circ})} \right) \\ &= \frac{1}{4} \frac{\tilde{P}(D_{\circ}, D_{\bullet})}{Q(D_{\circ}, D_{\bullet})Q(D_{\bullet}, D_{\circ})Q(1/D_{\circ}, 1/D_{\bullet})Q(1/D_{\bullet}, 1/D_{\circ})}. \end{split}$$

Hence F can be written as \tilde{P}/\tilde{Q} , where \tilde{P} and \tilde{Q} are two polynomials in D_{\circ} , D_{\bullet} , D_{\circ}^{-1} and D_{\bullet}^{-1} , which are both \parallel -symmetric and \times -symmetric. Therefore, both of them can be written as polynomials in t_{\circ}^{-1} and t_{\bullet}^{-1} , which implies that f is rational in t_{\circ} and t_{\bullet} and concludes the proof.

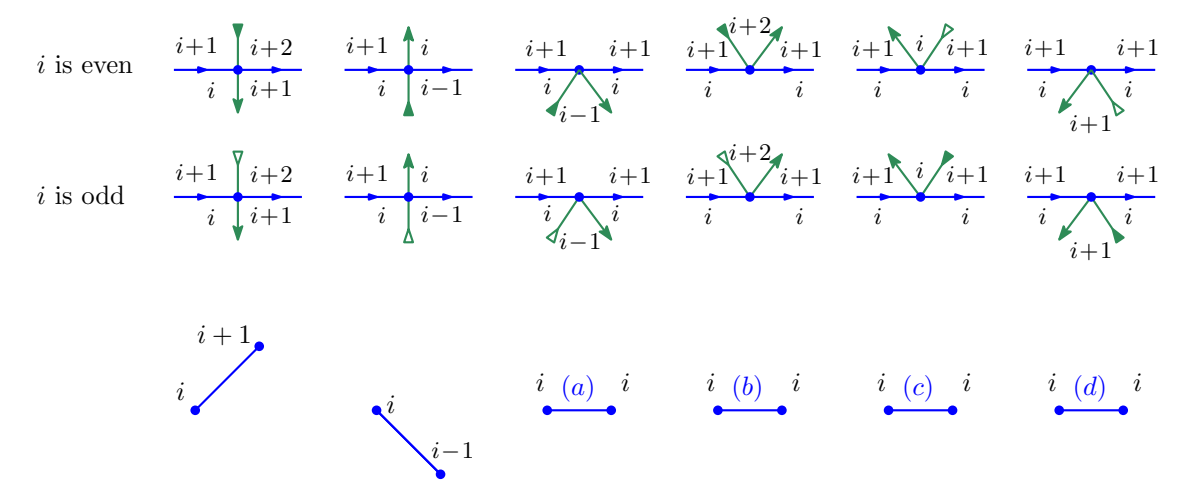


FIGURE 13. Illustration of the 6 types of branch vertices (top), the distinction between i even and odd enables us to indicate the color of the leaves on the branches. On the bottom, we represent the corresponding steps in the typed Motzkin paths where the heights of the vertices are indicated.

5. Rationality of the generating series of cores and schemes

5.1. Decomposition of cores according to their labeled scheme. For $\mathfrak{r} \in \mathcal{R}$, recall from Section 3.4.2 that, if \mathfrak{r} is well-oriented, then it induces an orientation on the edges of $\Theta(\mathfrak{r})$ that also makes it well-oriented. Additionally, if \mathfrak{r} is endowed with a labeling of its corners, we let corners of $\Theta(\mathfrak{r})$ inherit the labeling of their corresponding corners in \mathfrak{r} .

Definition 5.1. A rooted well-oriented blossoming scheme, equipped with a labeling of its corners, is called a labeled scheme if its root corner is labeled 0 and if the labels of adjacent corners incident to the same vertex differ by 1, and the corner with higher label is on the left of the separating half-edge.

The set of labeled schemes is denoted by \mathcal{L} .

It follows directly from the definition that if \mathfrak{r} is well-labeled, then $\Theta(\mathfrak{r}) \in \mathcal{L}$. As usual, for $\mathfrak{l} \in \mathcal{L}$, we denote by $\mathcal{R}_{\mathfrak{l}}$ the subset of elements of \mathcal{R} that admits \mathfrak{l} as labeled scheme. Note that a labeled scheme is not necessarily well-labeled because labels of corners adjacent along an edge may differ, see for instance Figure 14.

Remark 5.1. In Theorem 3.11, we grouped together "good maps" with the same unrooted core, thus obtaining a connection between the two generating series $O_{\bar{\mathfrak{r}}}^{\times}$ and $R_{\bar{\mathfrak{r}}}$, for any $\mathfrak{r} \in \mathcal{R}$. To apply the criterion given in Lemma 4.3, we go in a slightly different direction and now group together elements of \mathcal{R} which admit the same labeled scheme. For any $\mathfrak{l} \in \mathcal{L}$, it allows us to obtain in Lemma 5.4 a relatively explicit formula – as a function of D_{\circ} , D_{\bullet} and B – for the generating function $R_{\mathfrak{l}}$.

Fix $l \in \mathcal{L}$. To construct an element of \mathcal{R}_{l} from l, we need to replace each edge of l by a sequence of vertices of inner degree 2, in such a way that the labels around the scheme vertices after substitution coincide with the labels in the corners of l.

In an element of \mathcal{R} , the vertices of interior degree 2 can be of 6 different types, as illustrated in Figure 13 (top). When following a branch in the direction given by its orientation, the first type of vertex implies an increase of 1 in the labels, the second one a decrease of 1, and the last 4 do not change the value of the labels along the branch. Each of the latter ones is given a type in $\{a, b, c, d\}$, as described in Figure 13. Define the set of typed Motzkin paths to be the set of Motzkin walks such that each of their horizontal steps is decorated by a type in $\{a, b, c, d\}$.

For $e = \{u, v\} \in E(\mathfrak{l})$ oriented from u to v (in the canonical orientation of \mathfrak{l}), we denote respectively by $\lambda_{\mathfrak{l}}^{0}(e)$ and $\lambda_{\mathfrak{l}}^{1}(e)$ the labels of the corners on the right of u and respectively incident

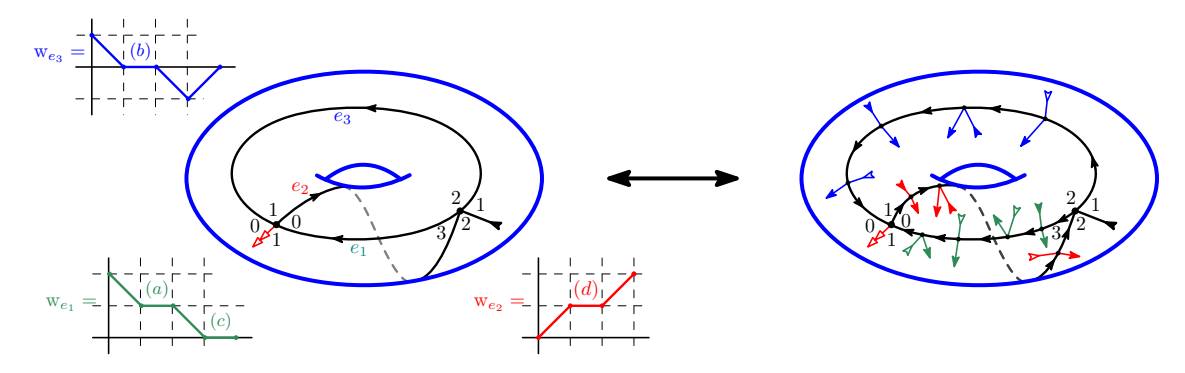


Figure 14. The correspondence between a decorated labeled scheme \mathfrak{l}^{\star} (left) and a blossoming core (right).

In this example, $\lambda_{\mathfrak{l}}^{0}(e_{1})=2$ and $\lambda_{\mathfrak{l}}^{1}(e_{1})=0$. Moreover, $E^{\uparrow}(\mathfrak{l})=\{e_{2}\}$ and $E^{\downarrow}(\mathfrak{l})=\{e_{1},e_{3}\}$.

to u and to v. In other words, $\lambda_{\mathfrak{l}}^{0}(e)$ (respectively $\lambda_{\mathfrak{l}}^{1}(e)$) is the label of the corner of \mathfrak{l} following e around u (respectively preceding e around v) in clockwise direction. For $\mathfrak{r} \in \mathcal{R}_{\mathfrak{l}}$, a branch with k edges in \mathfrak{r} corresponding to the edge e of \mathfrak{l} can then be encoded by a typed Motzkin walk of length k-1 starting at height $\lambda_{\mathfrak{l}}^{0}(e)$ and ending at height $\lambda_{\mathfrak{l}}^{1}(e)$. This justifies the following definition:

Definition 5.2. A decorated labeled scheme \mathfrak{l}^* is a couple $(\mathfrak{l}, (w_e)_{e \in E(\mathfrak{l})})$, such that $\mathfrak{l} \in \mathcal{L}$ and for each $e \in E(\mathfrak{l})$, w_e is a typed Motzkin path, that goes from height $\lambda_{\mathfrak{l}}^0(e)$ to height $\lambda_{\mathfrak{l}}^1(e)$.

The following fact is clear from the definitions:

Claim 5.3. The application that maps a decorated labeled scheme $\mathfrak{l}^* = (\mathfrak{l}, (w_e)_{e \in E(\mathfrak{l})})$ to a blossoming core, by replacing each edge $e \in E(\mathfrak{l})$ by the branch encoded by w_e is a bijection between decorated labeled schemes with \mathfrak{l} as labeled scheme and $\mathcal{R}_{\mathfrak{l}}$, see Figure 14.

To state the enumerative consequences of the preceding claim, we introduce a couple of additional notations. For an edge $e \in E(\mathfrak{l})$, e is said to be increasing (resp. decreasing) if $\lambda_{\mathfrak{l}}^{0}(e) \leq \lambda_{\mathfrak{l}}^{1}(e)$ (resp. $\lambda_{\mathfrak{l}}^{0}(e) > \lambda_{\mathfrak{l}}^{1}(e)$). The sets of increasing and decreasing edges of \mathfrak{l} are respectively denoted by $E^{\uparrow}(\mathfrak{l})$ and $E^{\downarrow}(\mathfrak{l})$. Furthermore, for $i, j \in \mathbb{N}$, we denote:

$$\Delta_i^j(x,y) \coloneqq x^{|[i,j[\cap (2\mathbb{Z})]}y^{|[i,j[\cap (2\mathbb{Z}+1)]} \quad \text{ for } i < j \qquad \text{ and } \qquad \Delta_i^i(x,y) = 1.$$

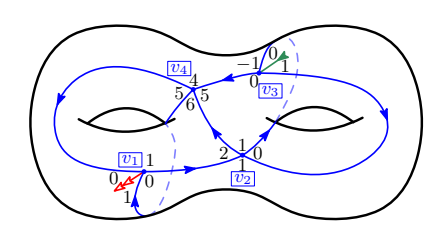
Lemma 5.4. For any $l \in \mathcal{L}$, we have the following equality:

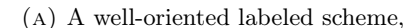
$$R_{\mathfrak{l}}(t_{\bullet},t_{\circ}) = \prod_{\sigma \in \mathcal{S}^{\rho}(\mathfrak{l})} \Delta_{\lambda_{\mathfrak{l}}(\sigma)}^{\lambda_{\mathfrak{l}}(\sigma)+1}(t_{\bullet},t_{\circ}) \cdot \prod_{e \in E^{\uparrow}(\mathfrak{l})} B \cdot \Delta_{\lambda_{\mathfrak{l}}^{0}(e)}^{\lambda_{\mathfrak{l}}^{1}(e)}(D_{\bullet},D_{\circ}) \cdot \prod_{e \in E^{\downarrow}(\mathfrak{l})} B \cdot \Delta_{\lambda_{\mathfrak{l}}^{1}(e)}^{\lambda_{\mathfrak{l}}^{0}(e)}(D_{\circ},D_{\bullet}),$$

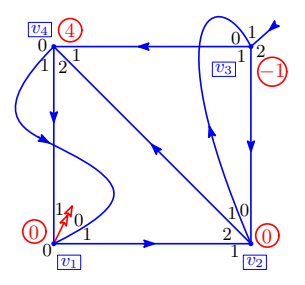
where we recall that $S^{\rho}(\mathfrak{l})$ denotes the rootable stems of \mathfrak{l} and that for $\sigma \in S^{\rho}(\mathfrak{l})$, $\lambda_{\mathfrak{l}}(\sigma)$ denotes its label as defined in Section 3.2.2.

Proof. Let $\mathfrak{l}^{\star} = (\mathfrak{l}, (\mathbf{w}_e))$ be a decorated labeled scheme. The rootable stems of $\phi(\mathfrak{l}, (\mathbf{w}_e))$ are either rootable stems of \mathfrak{l} or leaves created when replacing the edge e of \mathfrak{l} by the branch encoded by \mathbf{w}_e . It is clear from Figure 13 that for any $e \in E(\mathfrak{l})$:

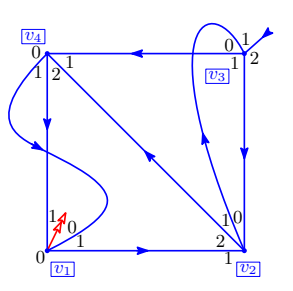
- each odd step of \mathbf{w}_e creates one white leaf in $\phi(\mathbf{l}, (\mathbf{w}_e))$,
- each even step of \mathbf{w}_e creates one black leaf in $\phi(\mathbf{l}, (\mathbf{w}_e))$,
- each horizontal step of w_e of type (a) or (b) creates one white leaf if i is odd (resp. one black leaf if i is even) in $\phi(\mathfrak{l}, (w_e))$
- each horizontal step of w_e of type (c) or (d) creates one black leaf if i is odd (resp. one white leaf if i is even) in $\phi(\mathfrak{l}, (w_e))$,







(B) with the height of its vertices and its relative labels.



(c) The corresponding unlabeled scheme.

FIGURE 15. Example of a well-oriented labeled scheme \mathfrak{l} of genus 2 with 4 vertices. In (A), \mathfrak{l} is represented classically on a torus of genus 2 with the labeling of its corners and its orientation. In (B) and (C), the same map is represented but the underlying surface is omitted.

In (B) and (C), corners are labeled by their relative labels (which could also be deduced from the canonical orientation of the edges). In (B), the height of each vertex is indicated by the circled red label. In (C), the corresponding unlabeled scheme is represented.

Recall the definition of the generating series $W^{i\to j}$ given in (5), we can then write:

$$R_{\mathfrak{l}}(t_{\bullet},t_{\circ}) = \prod_{\sigma \in \mathcal{S}^{\rho}(\mathfrak{l})} \Delta_{\lambda_{\mathfrak{l}}(\sigma)}^{\lambda_{\mathfrak{l}}(\sigma)+1}(t_{\circ},t_{\bullet}) \cdot \prod_{e \in E(\mathfrak{l})} W^{\lambda_{\mathfrak{l}}^{0}(e) \to \lambda_{\mathfrak{l}}^{1}(e)}(t_{\bullet},t_{\circ}).$$

Fix now $e \in E^{\downarrow}(\mathfrak{l})$, then a typed Motzkin path from $\lambda_{\mathfrak{l}}^{0}(e)$ to $\lambda_{\mathfrak{l}}^{1}(e)$ can be decomposed as a $(\lambda_{\mathfrak{l}}^{0}(e) - \lambda_{\mathfrak{l}}^{1}(e))$ -tuple of primitive typed Motzkin paths followed by a typed Motzkin bridge. It implies that for $e \in E^{\downarrow}(\mathfrak{l})$:

$$W^{\lambda_{\mathfrak{l}}^{0}(e) \to \lambda_{\mathfrak{l}}^{1}(e)}(t_{\bullet}, t_{\circ}) = B(t_{\bullet}, t_{\circ}) \prod_{k=\lambda_{\mathfrak{l}}^{1}(e)+1}^{\lambda_{\mathfrak{l}}^{0}(e)} W_{[\geq k]}^{k \to (k-1)}(t_{\bullet}, t_{\circ}),$$

Hence, for $e \in E^{\downarrow}(\mathfrak{l})$:

$$W^{\lambda_{\mathfrak{l}}^{0}(e) \to \lambda_{\mathfrak{l}}^{1}(e)}(t_{\bullet}, t_{\circ}) = B(t_{\bullet}, t_{\circ}) \cdot \Delta_{\lambda_{\mathfrak{l}}^{1}(e)}^{\lambda_{\mathfrak{l}}^{0}(e)}(D_{\circ}, D_{\bullet}).$$

A similar decomposition when e belongs to $E^{\uparrow}(\mathfrak{l})$ concludes the proof of the lemma.

Corollary 5.5. For any $l \in \mathcal{L}$, R_l is a rational function of D_{\bullet} and D_{\circ} .

Proof. Thanks to Lemma 5.4 and the expressions for t_{\bullet} and t_{\circ} given in (7) and (8), it is easy to see that $R_{\mathfrak{l}}$ is a rational function of B, D_{\circ} , and D_{\bullet} . Moreover, a little of algebra based on Property 4.1 and Equations (7) and (8) gives the following expression for B:

(9)
$$B = \frac{1 + 2(D_{\bullet} + D_{\circ}) + D_{\bullet}D_{\circ}}{1 - D_{\bullet}D_{\circ}},$$

so that $R_{\mathfrak{l}}$ is also rational as a function of D_{\bullet} and D_{\circ} only.

Since for a fixed genus, the number of labeled schemes is infinite, we explain in the next section how to further regrouping elements of \mathcal{R} , so as to be able to apply criterion of Lemma 4.3.

5.2. Unlabeled schemes, offset graphs and consistent namings. Let $l \in \mathcal{L}$ be a labeled scheme, then its *unlabeled scheme* – denoted us(l) – is (unsurprisingly) defined as the scheme obtained from l after erasing its labels. The set of unlabeled schemes of genus g is denoted \mathcal{S}_g .

5.2.1. Relative labels and height. Let $\mathfrak{l} \in \mathcal{L}$. For $v \in V(\mathfrak{l})$, the height $h_{\mathfrak{l}}(v)$ of v is defined as the minimum of the labels of its adjacent corners, i.e.:

$$h_{\mathfrak{l}}(v) = \min\{\lambda(\kappa), \text{ for } \kappa \text{ a corner incident to } v\}.$$

For $\kappa \in C(\mathfrak{l})$, the relative label of κ is set to be the difference $\lambda_l(\kappa) - h_{\mathfrak{l}}(v(\kappa))$, where $v(\kappa)$ denotes the vertex incident to κ . From the definition of a labeled scheme, observe that relative labels can also be retrieved from the orientation of the edges of \mathfrak{l} or of us(\mathfrak{l}). Therefore, it makes sense to speak of the relative labels of an unlabeled scheme and \mathfrak{l} can be reconstructed from us(\mathfrak{l}) and $(h_{\mathfrak{l}}(v))_{v \in V(\mathfrak{l})}$, see Figure 15.

The following fact will be useful in the sequel:

Claim 5.6. For $l \in \mathcal{L}$, the height of its root vertex is equal to 0.

Proof. From the definition of labeled scheme and of the labeling of corners of elements of \mathcal{R} , the only thing to prove is that the relative labels of the corners incident to the root vertex of \mathfrak{l} are all in $\{0,1\}$. Since \mathfrak{l} is well-oriented, the two edges following and preceding the root bud around its root vertex are necessarily oriented toward it, see Figure 15(A), which concludes the proof.

5.2.2. Types of half-edges. The definitions of this section are illustrated in Figure 16.

Let $\mathfrak{s} \in \mathcal{S}$, a half-edge of \mathfrak{s} is said to be of *type* 0 if it has adjacent relative labels 0 and 1, and of *type* 1 if it has adjacent relative labels 1 and 2. Since the relative labels of a 4-valent labeled scheme belong to $\{0,1,2\}$, a half-edge is either of type 0 or of type 1.

Definition 5.7 (balanced, shifted, and offset edges and stems). Fix $\mathfrak{s} \in \mathcal{S}$, an edge $\{u, v\}$ of \mathfrak{s} is said to be:

- balanced if it consists of two half-edges of type 0,
- shifted if it consists of two half-edges of type 1.
- offset toward v if it consists of a half-edge of type 0 on the side of u and a half-edge of type 1 on the side of v.

Similarly, a rootable stem is said to be:

- regular if it has adjacent relative labels 0 and 1,
- shifted if it has adjacent relative labels 1 and 2.

5.2.3. Consistent namings. Let $\mathfrak{s} \in \mathcal{S}$. A naming of \mathfrak{s} is a bijection from $V(\mathfrak{s})$ to $[|V(\mathfrak{s})|]$. A naming ν of \mathfrak{s} is called *consistent* if it is a linear extension of the partial order induced by the (acyclic) oriented graph of its offsets edges. In other words, a naming ν is consistent if, for any edge $\{u,v\}$ offset towards $v,\nu(u)<\nu(v)$.

The structure of the subgraph of \mathfrak{s} induced by its offset edges was investigated in [14], and the following result was obtained:

Theorem 5.8 (Theorem 4.14 of [14]). For any $\mathfrak{s} \in \mathcal{S}$, the directed graph of offset edges of \mathfrak{s} is acyclic.

As an immediate corollary we obtain:

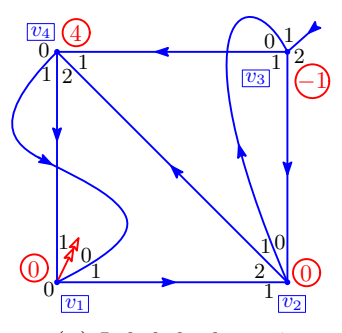
Corollary 5.9. Any $\mathfrak{s} \in \mathcal{S}$ admits a consistent naming.

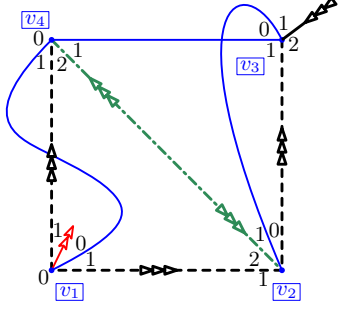
- 5.2.4. Height-order relative to a naming. Fix $\mathfrak{l} \in \mathcal{L}$, and let ν be a naming of us(\mathfrak{l}). The height order of \mathfrak{l} relative to ν is the bijection $\pi_{\mathfrak{l},\nu}: [|V(\mathfrak{s})|] \to V(\mathfrak{l})$ such that for any i < j:
 - Either $h_{\mathfrak{l}}(\pi_{\mathfrak{l},\nu}(i)) < h_{\mathfrak{l}}(\pi_{\mathfrak{l},\nu}(j)),$
 - Or $h_{\mathfrak{l}}(\pi_{\mathfrak{l},\nu}(i)) = h_{\mathfrak{l}}(\pi_{\mathfrak{l},\nu}(j))$ and $\nu(\pi_{\mathfrak{l},\nu}(i)) < \nu(\pi_{\mathfrak{l},\nu}(j))$.

In other words, $\pi_{\mathfrak{l},\nu}$ is the lexicographic order on the couple (height,naming). The inverse bijection $\pi_{\mathfrak{l},\nu}^{-1}:V(\mathfrak{l})\to[|V(\mathfrak{s})|]$ is called the *relative height* function.

Fix $\mathfrak{s} \in \mathcal{S}$, we denote by $\mathfrak{S}_{V(\mathfrak{s})}$ the set of bijections from $[|V(\mathfrak{s})|]$ to $V(\mathfrak{s})$. Let ν be a naming of \mathfrak{s} and $\pi \in \mathfrak{S}_{V(\mathfrak{s})}$. We denote by $\mathcal{L}^{\pi}_{\mathfrak{s},\nu}$ the set of labeled schemes with unlabeled scheme \mathfrak{s} , and height order relative to ν given by π . In other words:

$$\mathcal{L}^{\pi}_{\mathfrak{s},\nu} \coloneqq \{\mathfrak{l} \in \mathcal{L}_{\mathfrak{s}} | \pi_{\mathfrak{l},\nu} = \pi\}$$





(A) Labeled scheme I,

(B) and its unlabeled scheme $\mathfrak{s} := us(\mathfrak{l})$.

FIGURE 16. In (A) this is the labeled scheme \(\) of Figure 15(B). In (B), this is the corresponding unlabeled scheme, where its offset edges are represented by dashed black edges with a triple arrow illustrating the direction of offset, its shifted edge is represented as a dot-dashed green edge with two triple arrows, and its shifted stem as a black half edge with a triple arrow.

Let ν be the naming of $\mathfrak s$ defined by $\nu(v_i)=i$. Then, ν is consistent. Moreover, the height order $\pi_{\mathfrak l,\nu}$ of $\mathfrak l$ relative to ν is equal to $\pi_{\mathfrak l,\nu}(1)=v_3,\ \pi_{\mathfrak l,\nu}(2)=v_1,\ \pi_{\mathfrak l,\nu}(3)=v_2$ and $\pi_{\mathfrak l,\nu}(4)=v_4$.

Finally, we denote by $\mathcal{R}^{\pi}_{\mathfrak{s},\nu}$ the corresponding subset of \mathcal{R} :

(10)
$$\mathcal{R}^{\pi}_{\mathfrak{s},\nu} \coloneqq \bigcup_{\mathfrak{l}\in\mathcal{L}^{\pi}_{\mathfrak{s},\nu}} \mathcal{R}_{\mathfrak{l}}.$$

5.3. Mirror operation and its consequences.

Definition 5.10 (mirror ordering). Fix $\mathfrak{s} \in \mathcal{S}$ and $\pi \in \mathfrak{S}_{V(\mathfrak{s})}$. The mirror of π , denoted $\overline{\pi}$, is the bijection such that, for any $k \in [|V(\mathfrak{s})|]$:

(11)
$$\overline{\pi}(k) = \pi(|V(\mathfrak{s})| + 1 - k).$$

In other words, if we set $\overline{k} := |V(\mathfrak{s})| + 1 - k$, then we have $\overline{\pi}(k) = \pi(\overline{k})$. Note that the mirror operation is an involution, i.e. $\overline{\overline{\pi}} = \pi$.

The mirror operation allows us to state this refined rationality scheme which is key in combinatorial proof of Theorem 1.2:

Theorem 5.11. For any $\mathfrak{s} \in \mathcal{S}$, any consistent naming ν of \mathfrak{s} and any $\pi \in \mathfrak{S}_{V(\mathfrak{s})}$, we have:

$$\overline{R_{\mathfrak{s},\nu}^{\pi}(D_{\bullet},D_{\circ})}^{\parallel} + \overline{R_{\mathfrak{s},\nu}^{\pi}(D_{\circ},D_{\bullet})}^{\parallel} = R_{\mathfrak{s},\nu}^{\overline{\pi}}(D_{\bullet},D_{\circ}) + R_{\mathfrak{s},\nu}^{\overline{\pi}}(D_{\circ},D_{\bullet}).$$

Moreover, $R_{\mathfrak{s},\nu}^{\pi}(D_{\bullet},D_{\circ})$ is a rational function of D_{\bullet} and D_{\circ} .

Hence, by Lemma 4.3, $R_{\mathfrak{s},\nu}(t_{\bullet},t_{\circ}) + R_{\mathfrak{s},\nu}(t_{\circ},t_{\bullet})$ is a rational function of t_{\bullet} and t_{\circ} .

We obtain as an immediate corollary:

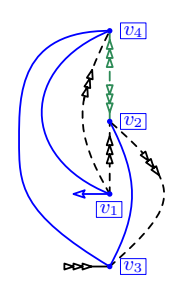
Corollary 5.12. For any $\mathfrak{s} \in \mathcal{S}$, the series $R_{\mathfrak{s}}^{\mathfrak{o}}(D_{\bullet}, D_{\circ}) := R_{\mathfrak{s}}(D_{\bullet}, D_{\circ}) + R_{\mathfrak{s}}(D_{\circ}, D_{\bullet})$ is a rational function of D_{\bullet} and D_{\circ} , and is \parallel -symmetric as a function of D_{\bullet} and D_{\circ} .

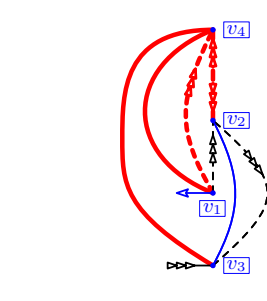
Proof. Let \mathfrak{s} be an unlabeled scheme. By Corollary 5.9, \mathfrak{s} admits a consistent naming, and let ν be such a naming. Then:

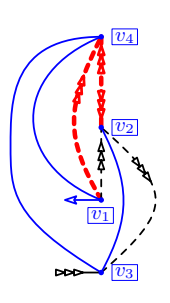
$$R_{\mathfrak{s}} = \sum_{\pi \in \mathfrak{S}_{V(\mathfrak{s})}} R_{\mathfrak{s},\nu}^{\pi}.$$

It follows directly from Theorem 5.11 that:

$$\overline{R_{\mathfrak{s}}^{\mathbf{0}}}^{\parallel} = \left(\sum_{\pi \in \mathfrak{S}_{V(\mathfrak{s})}} R_{\mathfrak{s}}^{\overline{\pi}}\right)^{\mathbf{0}} = R_{\mathfrak{s}}^{\mathbf{0}},$$









(A) The unlabeled scheme \mathfrak{s} as a graph.

(B) Edges positively enclosing relative height 3.

(c) Edges which overfit at relative height 4.

(D) Shifted buds.

FIGURE 17. In (A), the unlabeled scheme $\mathfrak s$ of Figure 16(B) is represented as a graph, and its vertices are ordered with respect to their preimage by π , where $\pi \in \mathfrak S_{V(\mathfrak s)}$ is defined by $\pi(1) = v_3$, $\pi(2) = v_1$, $\pi(3) = v_2$ and $\pi(4) = v_4$. The orientation of the edges and the relative labels of the corners are not represented, but the offset and shifted edges and the shifted buds remain distinguished. This suffices to compute all the statistics of Section 5.4.

We see from (A), that ν and π are discordant at relative height 1 and concordant otherwise. In (B) the edges that are positively enclosing at relative height 3 are represented by fat red dashed edges, so that $C_{\mathfrak{s}}^{\pi,3:+}=4$. In (C) the edges that overfit at relative height 4 are represented by fat red dashed edges, so that $O_{\mathfrak{s}}^{\pi,4}=2$. In (D), the shifted buds are represented by fat red edges with triple arrow, so that $B_{\mathfrak{s}}^{\pi,1:+}=1$ and $B_{\mathfrak{s}}^{\pi,2}=1$.

where the last equality comes from the fact that the mirror operation is a bijection on $\mathfrak{S}_{V(\mathfrak{s})}$. \square

The proof of Theorem 5.11 will be the purpose of the next two sections but we first explain why it concludes the bijective proof of Theorem 1.2.

For $\mathfrak{s} \in \mathcal{S}$, its unrooted map (recall Definition 3.10) is called an *unrooted scheme*, and the set of unrooted schemes is denoted by $\overline{\mathcal{S}}$. As before, for any $\mathfrak{u} \in \overline{\mathcal{S}}$, we denote by $M_{\mathfrak{u}}(z_{\bullet}, z_{\circ})$ the generating series of maps which correspond to the unrooted scheme \mathfrak{u} . In other words, the image of these maps by the bijection given in Corollary 3.8 are good maps that admit \mathfrak{u} as unrooted scheme.

Theorem 5.13. For any unrooted scheme $\mathfrak{u} \in \overline{\mathcal{S}}$, the generating series $M_{\mathfrak{u}}(z_{\bullet}, z_{\circ})$ is a rational function of the series T_{\bullet} and T_{\circ} defined in (2).

Hence, $M_q(z_{\bullet}, z_{\circ})$ is also a rational function of T_{\bullet} and T_{\circ} .

Proof. Lemma 4.3 and Corollary 5.12 directly imply that the series $R_{\mathfrak{s}}^{\bullet}$ is a rational function of t_{\circ} and t_{\bullet} . Fix now \mathfrak{u} in $\bar{\mathcal{S}}$. The number of unlabeled schemes that admit \mathfrak{u} as unrooted scheme is equal to $2q - |\mathring{n}_2(\mathfrak{u})|$ and is hence finite. It implies that $R_{\mathfrak{s}}^{\bullet}$ is also rational as a series in t_{\circ} and t_{\bullet} .

equal to $2g - |\mathring{n}_2(\mathfrak{u})|$ and is hence finite. It implies that $R^{\bullet}_{\mathfrak{u}}$ is also rational as a series in t_{\circ} and t_{\bullet} . By Theorem 3.11, we deduce that $O^{\times}_{\mathfrak{u}}$ is rational in T_{\circ} and T_{\bullet} . And finally, by Corollary 3.8, we conclude that $M_{\mathfrak{u}}$ is a rational function of T_{\circ} and T_{\bullet} . Since the number of unrooted schemes of genus g is finite, it implies that $M_g(z_{\bullet}, z_{\circ})$ is also a rational function of T_{\bullet} and T_{\circ} , which concludes the proof.

5.4. Statistics on unlabeled schemes. We gather in this section some definitions of a few statistics on unlabeled schemes, that are illustrated on Figure 17. These statistics allow to capture the error made when replacing the label of a corner by the height of its incident corner. Thanks to them, we can obtain nice closed formulas for $R_{s,\nu}^{\pi}$, that will be stated in Lemmas 6.3 and 7.4 and that will be key in the proof of Theorem 5.11.

This section, which is technical and quite cumbersome (despite our best efforts), can be first skipped and the reader can then looked up the definitions as needs be.

In all this section, \mathfrak{s} is a fixed element of \mathcal{S} , ν is a naming of its vertices, π is an element of $\mathfrak{S}_{V(\mathfrak{s})}$, and k lies in $[|V(\mathfrak{s})|]$

Definition 5.14 (naming-ordering discordance indicator at a relative height). The naming ν and the ordering π are said to be concordant at relative height k if $\nu(\pi(k+1)) > \nu(\pi(k))$, and discordant otherwise, see Figure 17(A).

The naming-ordering discordance indicator at relative height k, denoted $\delta_{\mathfrak{s},\nu}^{\pi,k:+}$ (or $\delta_{\mathfrak{s},\nu}^{\pi,(k+1):-}$), is defined as being 1 if ν and π are discordant at relative height k, and 0 otherwise. In other words:

(12)
$$\delta_{\mathfrak{s},\nu}^{\pi,k:+} = \delta_{\mathfrak{s},\nu}^{\pi,(k+1):-} = \begin{cases} 1 & \text{if } \nu(\pi(k+1)) \leq \nu(\pi(k)) \\ 0 & \text{otherwise.} \end{cases}$$

Let $\mathfrak{l} \in \mathcal{L}^{\pi}_{\mathfrak{s},\nu}$. Then $h_{\mathfrak{l}}(\pi(k+1)) \geq h_{\mathfrak{l}}(\pi(k)) + \delta^{\pi,k:+}_{\mathfrak{s},\nu}$. Indeed, by definition of the relative height order: $h_{\mathfrak{l}}(\pi(k+1)) \geq h_{\mathfrak{l}}(\pi(k))$, where the case of equality can only occur if $\nu(\pi(k+1)) > \nu(\pi(k))$, i.e. if ν and π are concordant at relative height k.

Definition 5.15 (edge enclosing a relative height). An edge $\{u,v\} \in E(\mathfrak{s})$ is said to be positively enclosing relative height k (see Figure 17(B)) if

- either $\pi^{-1}(u) \le k < \pi^{-1}(v)$,
- or $\pi^{-1}(v) \le k < \pi^{-1}(u)$.

Symmetrically, $\{u,v\}$ is said to be negatively enclosing relative height k if

- either $\pi^{-1}(u) < k \le \pi^{-1}(v)$, or $\pi^{-1}(v) < k \le \pi^{-1}(u)$.

The number of edges positively enclosing relative height k (respectively negatively) is denoted $C_5^{\pi,k:+}$ (respectively $C_{\mathfrak{s}}^{\pi,k:-}$).

- Note that: $\mathsf{C}_{\mathfrak{s}}^{\pi,1^-} = \mathsf{C}_{\mathfrak{s}}^{\pi,|V(\mathfrak{s})|:+} = 0$
 - for any $k \in [|V(\mathfrak{s})|-1]$, $C_{\mathfrak{s}}^{\pi,k:+} = C_{\mathfrak{s}}^{\pi,(k+1):-}$

Definition 5.16 (overfitting and underfitting edges). An edge $e = \{u, v\} \in E(\mathfrak{s})$ is overfitting (respectively underfitting) at relative height k (see Figure 17(C)) if:

- $\pi^{-1}(v) = k \text{ and } \pi^{-1}(u) < k \text{ (respectively } \pi^{-1}(u) > k),$
- and, e is either offset towards v or shifted.

We denote by $\mathfrak{of}_{\mathfrak{s}}^{\pi,k}: E(\mathfrak{s}) \to \{0;1\}$ (respectively $\mathfrak{uf}_{\mathfrak{s}}^{\pi,k}: E(\mathfrak{s}) \to \{0;1\}$) the function that associates 1 to an edge overfitting (respectively underfitting) at relative height k, and 0 to other edges.

The overfit (respectively underfit) of \mathfrak{s} at relative height k, denoted $\mathfrak{O}_{\mathfrak{s}}^{\pi,k}$ (respectively $\mathfrak{U}_{\mathfrak{s}}^{\pi,k}$), is the number of overfitting (respectively underfitting) edges of $\mathfrak s$ at relative height k. In other words:

$$\mathtt{O}_{\mathfrak{s}}^{\pi,k} = \sum_{e \in E(\mathfrak{s})} \mathtt{of}_{\mathfrak{s}}^{\pi,k}(e) \quad \text{ and } \quad \mathtt{U}_{\mathfrak{s}}^{\pi,k} \coloneqq \sum_{e \in E(\mathfrak{s})} \mathtt{uf}_{\mathfrak{s}}^{\pi,k}(e).$$

The total overfit and total underfit of \mathfrak{s} - denoted respectively $\mathfrak{Q}^\pi_{\mathfrak{s}}$ and $\mathfrak{V}^\pi_{\mathfrak{s}}$ - is the number of overfitting and underfitting edges of \mathfrak{s} .

Note that $O_{\mathfrak{s}}^{\pi,1} = U_{\mathfrak{s}}^{\pi,|V(\mathfrak{s})|} = 0$. Note also that any offset edge either overfits or underfits at a unique relative height and that any shifted edge overfits at a unique relative height and underfits at a unique relative height.

Definition 5.17 (number of regular and shifted buds at a relative height). *The* number of regular (respectively shifted) buds at relative height k, denoted $B_5^{\pi,k}$ (respectively $B_5^{\pi,k+}$), is the number of regular (respectively shifted) buds of \mathfrak{s} incident to the vertex $\pi(k)$.

In a 4-valent scheme, there is at most one bud per scheme vertex. By consequence, $B_{\mathfrak{s}}^{\pi,k} + B_{\mathfrak{s}}^{\pi,k:+}$ is either 1 if there is a bud incident to the vertex of relative height k, and 0 otherwise.

The different statistics defined above behave well with respect to the mirror operation, as stated in the following proposition, which follows directly from the definitions:

Proposition 5.18. Fix $\mathfrak{s} \in \mathcal{S}$, $\pi \in \mathfrak{S}_{V(\mathfrak{s})}$, $k \in [|V(\mathfrak{s})|]$, and $e \in E(m)$.

$$\begin{array}{ll} \mathbf{C}_{\mathfrak{s}}^{\overline{\pi},k:+} = \mathbf{C}_{\mathfrak{s}}^{\pi,\overline{k}:-} & \mathbf{D}_{\mathfrak{s}}^{\overline{\pi},k} = \mathbf{U}_{\mathfrak{s}}^{\pi,\overline{k}} \\ \\ \mathbf{of}_{\mathfrak{s}}^{\overline{\pi},k}(e) = \mathbf{uf}_{\mathfrak{s}}^{\pi,\overline{k}}(e) & \mathbf{D}_{\mathfrak{s}}^{\overline{\pi}} = \mathbf{U}_{\mathfrak{s}}^{\pi} & \mathbf{B}_{\mathfrak{s}}^{\overline{\pi},k:+} = \mathbf{B}_{\mathfrak{s}}^{\pi,\overline{k}:+} \\ \end{array}$$

Moreover, for any naming ν of \mathfrak{s} , we have:

$$\delta_{\mathfrak{s},\nu}^{\overline{\pi},k:+} = 1 - \delta_{\mathfrak{s},\nu}^{\pi,\overline{k}:-}$$

6. The univariate case: Proof of Theorem 1.1

As a warm-up, we first now prove a univariate version of Theorem 5.11, which gives a simpler combinatorial proof of Theorem 1.1 as the one obtained in [14].

In this section, all the generating series considered are assumed to be univariate. But, with a slight abuse of notation, we keep the same notation. So that, for instance $R_{\mathfrak{s}}(t) := R_{\mathfrak{s}}(t,t)$, $D(t) := D_{\mathfrak{o}}(t,t) = D_{\mathfrak{o}}(t,t)$, B(t) := B(t,t) and $T(z) := T_{\mathfrak{o}}(z,z) = T_{\mathfrak{o}}(z,z)$. Moreover, for any function f of D, we set $\overline{f}^{\parallel}(D) := f(1/D)$.

We hence prove in this section the following univariate specialization of Theorem 5.11:

Theorem 6.1. Let $\mathfrak{s} \in \mathcal{S}$, ν be a naming of its vertices, and $\pi \in \mathfrak{S}_{V(\mathfrak{s})}$. Then $R^{\pi}_{\mathfrak{s},\nu}$ is a rational function of D, and we have the following identity:

$$\overline{R_{\mathfrak{s},\nu}^{\overline{\pi}}}^{\parallel}(D) = R_{\mathfrak{s},\nu}^{\pi}(D).$$

As in Section 5.3, it gives as an immediate corollary:

Corollary 6.2. For any unlabeled scheme $\mathfrak{s} \in \mathcal{S}$, the series $R_{\mathfrak{s}}(t) := R_{\mathfrak{s}}(t,t)$ is rational and symmetric in D(t) and $D(t)^{-1}$, where $D(t) := D_{\bullet}(t,t) = D_{\bullet}(t,t)$.

Note that a proof of Corollary 6.2 is already given in [14], but we give here a different proof that we were able to extend to the general case. The differences between the two proofs will be discussed in Remark 6.1. Using a univariate version of Lemma 4.3 due to [8], Corollary 6.2 can be used to prove the rationality of $M_g(z)$, thus giving a combinatorial proof of Theorem 1.1.

To give the proof of Theorem 6.1, we first obtain an explicit formula for the generating series $R_{\mathfrak{s},\nu}^{\pi}$. We denote by bR the generating series of \mathcal{R} , where the weight of scheme stems is set to 0, so that only leaves on a branch are taken into consideration. This is still a valid generating function since there is only a (fixed) finite number of stems on a given scheme. We define similarly the generating series ${}^bR_{\mathfrak{s},\nu}^{\pi}$ and ${}^bR_{\mathfrak{l}}$ of the corresponding subfamilies of \mathcal{R} . Then, we have:

Lemma 6.3. Fix $\mathfrak{s} \in \mathcal{S}$, ν a consistent naming of \mathfrak{s} , and $\pi \in \mathfrak{S}_{V(\mathfrak{s})}$, then:

$${}^b\!R^\pi_{\mathfrak{s},\nu} = B^{|E(\mathfrak{s})|} \cdot D^{\mathfrak{0}^\pi_{\mathfrak{s}} - \mathfrak{U}^\pi_{\mathfrak{s}}} \cdot \prod_{k \in [|V(\mathfrak{s})| - 1]} \frac{D^{\delta^{\pi,k:+}_{\mathfrak{s},\nu} \cdot \mathbb{C}^{\pi,k:+}_{\mathfrak{s}}}}{1 - D^{\mathbb{C}^{\pi,k:+}_{\mathfrak{s}}}},$$

where $C_{\mathfrak{s}}^{\pi,k:+}$, $O_{\mathfrak{s}}^{\pi,k}$, $U_{\mathfrak{s}}^{\pi,k}$, and $\delta_{\mathfrak{s},\nu}^{\pi,k:+}$ are defined in Definitions 5.14 to 5.16.

Proof. By decomposing the family of maps $\mathcal{R}^{\pi}_{\mathfrak{s},\nu}$ according to their labeled scheme, we get:

$${}^b\!R^\pi_{\mathfrak{s},\nu} = \sum_{\mathfrak{l}\in\mathcal{L}^\pi_{\mathfrak{s},\nu}} {}^b\!R_{\mathfrak{l}}$$

For a given labeled scheme \mathfrak{l} , the generating series ${}^{b}R_{\mathfrak{l}}$ can be easily computed as the product of the contribution of the branches of \mathfrak{l} , thanks to Lemma 5.4. For $e \in E(\mathfrak{l})$, recall the definition of $\lambda_{\mathfrak{l}}^{0}(e)$ and $\lambda_{\mathfrak{l}}^{1}(e)$ from Section 5.1, then we define the *statute* of e – denoted $\Delta(e)$ – by:

$$\Delta(e) = |\lambda_{\rm I}^0(e) - \lambda_{\rm I}^1(e)|.$$

Setting $D_{\bullet} = D_{\circ}$ in Lemma 5.4 and ignoring the contribution of the scheme rootable stems, we get:

$${}^b\!R_{\mathfrak{l}} = \prod_{e \in E(\mathfrak{l})} B \cdot D^{\Delta(e)}.$$

The stature of an edge $\{u, v\}$ depends only on the heights $h_{\mathfrak{l}}(u)$ and $h_{\mathfrak{l}}(v)$, and whether e is offset or not. Namely:

$$\Delta(\lbrace u, v \rbrace) = |h_{\mathfrak{l}}(u) - h_{\mathfrak{l}}(v)| + \epsilon_{\mathfrak{l}}(\lbrace u, v \rbrace),$$

where:

(13)
$$\epsilon_{\mathfrak{l}}(\{u,v\}) = \begin{cases} 0, & \text{if } \{u,v\} \text{ is not offset} \\ 1, & \text{if } \{u,v\} \text{ is offset toward } v \text{ and } h_{\mathfrak{l}}(v) \geq h_{\mathfrak{l}}(u) \\ -1, & \text{if } \{u,v\} \text{ is offset toward } v \text{ and } h_{\mathfrak{l}}(v) < h_{\mathfrak{l}}(u) \end{cases}.$$

Recall the definition of $R_{\mathfrak{s},\nu}^{\pi}$ given in (10), then:

$${}^b\!R^\pi_{\mathfrak{s},\nu} = B^{|E(\mathfrak{s})|} \cdot \sum_{\mathfrak{l} \in \mathcal{L}^\pi_{\mathfrak{s},\nu}} \prod_{\substack{\mathfrak{q} = \mathfrak{q}(u,v) \in E(\mathfrak{l}) \\ \pi^{-1}(u) < \pi^{-1}(v)}} D^{h_{\mathfrak{l}}(v) - h_{\mathfrak{l}}(u) + \epsilon_{\mathfrak{l}}(\{u,v\})}.$$

For $\mathfrak{s} \in \mathcal{S}$ fixed, together with a naming ν and $\pi \in \mathfrak{S}_{V(\mathfrak{s})}$, an element \mathfrak{l} of $\mathcal{L}^{\pi}_{\mathfrak{s},\nu}$ is fully characterized by a sequence $(h_k)_{k \in [|V(\mathfrak{s})|]}$, where for any $k \in [|V(\mathfrak{s})|]$, h_k gives the height of $\pi(k)$ in \mathfrak{l} . Since \mathfrak{l} belongs to $\mathcal{L}^{\pi}_{\mathfrak{s},\nu}$, by Claim 5.6, the height of the root vertex of \mathfrak{l} must be equal to 0 and, furthemore, this sequence must satisfy:

$$\begin{cases} h_{k+1} \ge h_k & \text{if } \nu(\pi(k+1)) > \nu(\pi(k)) \\ h_{k+1} > h_k & \text{otherwise.} \end{cases}$$

In other words:

$$(14) h_{k+1} \ge h_k + \delta_{\mathfrak{s},\nu}^{\pi,k:+}.$$

Alternatively, by a change of variable, a labeled scheme $\mathfrak{l} \in \mathcal{L}^{\pi}_{\mathfrak{s},\nu}$ is characterized by the sequence $(I_k)_{k \in [|V(\mathfrak{s})|-1]} = (h_{k+1}-h_k)_{k \in [|V(\mathfrak{s})|-1]}$ of the differences between successive heights of the vertices $\pi(k)$ in \mathfrak{l} . By (14), such a sequence must satisfy

$$I_k \geq \delta_{\mathfrak{s},\nu}^{\pi,k:+} \text{ for any } k \in [|V(\mathfrak{s})|-1].$$

We denote by $\mathcal{I}^{\pi}_{\mathfrak{s},\nu}$ the set of such sequences. Then:

$${}^{b}R_{\mathfrak{s},\nu}^{\pi} = B^{|E(\mathfrak{s})|} \cdot \sum_{\substack{(I_{k}) \in \mathcal{I}_{\mathfrak{s},\nu}^{\pi} \\ \pi^{-1}(u) < \pi^{-1}(v)}} D^{I_{\pi^{-1}(u)} + \dots + I_{\pi^{-1}(v)-1} + \epsilon_{\mathfrak{l}}(\{u,v\})},$$

and by (13) and Definition 5.15:

$${}^b\!R_{\mathfrak{s},\nu}^\pi = B^{|E(\mathfrak{s})|} \cdot \sum_{(I_k) \in \mathcal{I}_{\mathfrak{s},\nu}^\pi} \prod_{k \in [|V(\mathfrak{s})|-1]} D^{I_k \cdot \mathsf{C}_{\mathfrak{s}}^{\pi,k:+}} \cdot \prod_{\{u,v\} \in E(\mathfrak{l})} D^{\epsilon_{\mathfrak{l}}(\{u,v\})}.$$

Let $\{u,v\}$ be an edge of \mathfrak{s} offset toward v. Since ν is consistent and by definition of $\mathcal{L}^{\pi}_{\mathfrak{s},\nu}$, $h_{\mathfrak{l}}(v) \geq h_{\mathfrak{l}}(u)$ if and only if $\pi^{-1}(u) < \pi^{-1}(v)$. We emphasize that the equality case of this equivalence is in fact the only part of the proof of Corollary 6.2 where we use the fact that ν is consistent. Consequently, for any $\{u,v\}$ offset toward v, we get, by Definition 5.16:

$$\epsilon_{\mathfrak{l}}(\{u,v\}) = \begin{cases} 1 & \text{if } \{u,v\} \text{ overfits at relative height } \pi^{-1}(v), \\ -1 & \text{if } \{u,v\} \text{ underfits at relative height } \pi^{-1}(v). \end{cases}$$

Since any shifted edge contributes once to $\mathbb{Q}_{\mathfrak{s}}^{\pi}$ and once to $\mathbb{Q}_{\mathfrak{s}}^{\pi}$, we finally get, by Definition 5.16:

$$\sum_{\{u,v\}\in E(\mathfrak{l})} \epsilon_{\mathfrak{l}}(\{u,v\}) = \mathbf{0}_{\mathfrak{s}}^{\pi} - \mathbf{U}_{\mathfrak{s}}^{\pi}.$$

Therefore:

$${}^bR^\pi_{\mathfrak{s},\nu} = B^{|E(\mathfrak{s})|} \cdot D^{\mathbf{0}^\pi_{\mathfrak{s}} - \mathbf{U}^\pi_{\mathfrak{s}}} \cdot \sum_{(I_k) \in \mathcal{I}^\pi_{\mathfrak{s},\nu}} \prod_{k \in [|V(\mathfrak{s})| - 1]} D^{I_k \cdot \mathbf{C}^{\pi,k:+}_{\mathfrak{s}}}$$

and finally, as claimed:

$${}^b\!R^\pi_{\mathfrak{s},\nu} = B^{|E(\mathfrak{s})|} \cdot D^{\mathfrak{0}^\pi_{\mathfrak{s}} - \mathsf{U}^\pi_{\mathfrak{s}}} \cdot \prod_{k \in [|V(\mathfrak{s})| - 1]} \frac{D^{\delta^{\pi,k:+}_{\mathfrak{s},\nu} + \cdot \mathsf{C}^{\pi,k:+}_{\mathfrak{s}}}}{1 - D^{\mathsf{C}^{\pi,k:+}_{\mathfrak{s}}}}.$$

Proof of Theorem 6.1. Since t and B are rational functions of D, the definition of ${}^bR^{\pi}_{\mathfrak{s},\nu}$ and Lemma 6.3 imply that $R^{\pi}_{\mathfrak{s},\nu}$ is also rational in D. Moreover, by Lemma 6.3, we have:

$$\overline{{}^b\!R_{\mathfrak{s},\nu}^{\overline{\pi}}} = \overline{B^{|E(\mathfrak{s})|} \cdot D^{\mathfrak{0}_{\mathfrak{s}}^{\pi} - \mathsf{U}_{\mathfrak{s}}^{\pi}} \cdot \prod_{k \in [|V(\mathfrak{s})| - 1]} \frac{D^{\delta_{\mathfrak{s},\nu}^{\pi,k:+} \cdot \mathsf{C}_{\mathfrak{s}}^{\pi,k:+}}}{1 - D^{\mathsf{C}_{\mathfrak{s}}^{\pi,k:+}}}.$$

It follows from (9), that $\overline{B} = -B$ and hence:

$$\overline{{}^b\!R^{\overline{\pi}}_{\mathfrak{s},\nu}} = (-B)^{|E(\mathfrak{s})|} \cdot D^{-\mathbf{0}^\pi_{\mathfrak{s}} + \mathbf{U}^\pi_{\mathfrak{s}}} \cdot \prod_{k \in [|V(\mathfrak{s})|-1]} \frac{D^{-\delta^{\pi,k:+}_{\mathfrak{s},\nu} + .\mathsf{c}^{\pi,k:+}_{\mathfrak{s}}}}{1 - D^{-\mathsf{c}^{\pi,k:+}_{\mathfrak{s}}}}.$$

We apply the change of variable $\overline{k} := |V(\mathfrak{s})| + 1 - k$, and obtain, by Proposition 5.18:

$$\begin{split} \overline{{}^b\!R^{\overline{\pi}}_{\mathfrak{s},\nu}} &= (-1)^{|E(\mathfrak{s})|} B^{|E(\mathfrak{s})|} \cdot D^{-\mathtt{U}^{\overline{\pi}}_{\mathfrak{s}} + \mathtt{O}^{\overline{\pi}}_{\mathfrak{s}}} \cdot \prod_{k \in [|V(\mathfrak{s})| - 1]} \frac{D^{(\bar{\delta}^{\overline{\pi},\overline{k}:-}_{\mathfrak{s},\nu} - 1) \cdot \mathtt{C}^{\overline{\pi},\overline{k}:-}_{\mathfrak{s}}}}{1 - D^{-\mathtt{C}^{\overline{\pi},\overline{k}:-}_{\mathfrak{s}}}} \\ \overline{{}^b\!R^{\overline{\pi}}_{\mathfrak{s},\nu}} &= (-1)^{|E(\mathfrak{s})| + |V(\mathfrak{s})| - 1} \cdot {}^b\!R^{\pi}_{\mathfrak{s},\nu}. \end{split}$$

Since \mathfrak{s} is a unicellular map of an orientable surface, by Euler's formula, we get $(-1)^{|E(\mathfrak{s})|+|V(\mathfrak{s})|-1} = 1$. Hence:

$$\overline{{}^b}\overline{R}_{\mathfrak{s},\nu}^{\overline{\pi}} = {}^bR_{\mathfrak{s},\nu}^{\pi}.$$

From (7) and (8) of Section 4.2, it is easy to see that, as a function of D, $\bar{t} = t$. Hence reincorporating the weights of the scheme stems in $b\overline{R}_{\bar{s},\nu}^{\overline{m}}$ gives:

$$\overline{R^{\overline{\pi}}_{\mathfrak{s},\nu}} = R^{\pi}_{\mathfrak{s},\nu},$$

which concludes the proof.

Remark 6.1. Note that the proof presented in this section differs from the one given in [14]. In the former, the schemes are also grouped by relative ordering of the height of their vertices. However, unlike here, where the equality cases of the relative ordering are resolved using a consistent naming of the vertices so as to obtain a bijection, the relative ordering in [14] is represented by a surjection. It results in some alternated sum on surjections, that end up canceling out after a careful analysis on the structure of surjections. Note also that this additional work include the definition of a so-called *canonical bijection* as a representative of a set of surjection, which can be seen as a very close analogous of the choice of a consistent labeling and the present definition of the relative ordering.

This bijection-grouping of schemes seems to be an overall better way of understanding the structure of schemes. Indeed, the expressions obtained are simpler, and in particular do not involve alternated sums, which is more satisfying from a bijective point of view. On a more pragmatic level, we were also not able to extend the original proof of [14] to the bivariate setting.

7. The bivariate case: Combinatorial proof of Theorem 5.12

7.1. Binary bijections.

7.1.1. Definition. In the bivariate case, the weight of a branch in a labeled scheme depends not only on the stature of the corresponding edge, but also on the parity of its labels. For this reason, we introduce binary bijections, that allow to sort labeled schemes not only by the relative ordering of their vertices, but also by the parity of the difference of heights between any pair of vertices.

Unlike in the univariate case developed in the previous section, giving a closed formula for the bivariate series of cores characterized by a given binary bijection is more complex. So instead of a bivariate analogue of Lemma 6.3, we give a recursive description of that series.

To do so, some additional terminology is needed. For $\mathfrak{s} \in \mathcal{S}$, a binary bijection of \mathfrak{s} is a couple $(\pi,\zeta) \in \mathfrak{S}_{V(\mathfrak{s})} \times (\mathbb{Z}/2\mathbb{Z})^{[|V(\mathfrak{s})|-1]}$. The set of binary bijections associated to \mathfrak{s} is denoted $\mathcal{BB}_{\mathfrak{s}}$. Fix ν a consistent naming of \mathfrak{s} . For $\mathfrak{l} \in \mathcal{L}$, such that us(\mathfrak{l}) = \mathfrak{s} , the binary bijection of \mathfrak{l} with respect to ν is the couple made of $\pi_{\mathfrak{l},\nu}$ – its height order relative to ν – and the function:

$$\zeta_{\mathfrak{l},\nu}:[|V(\mathfrak{s})|-1]\to \mathbb{Z}/2\mathbb{Z}\quad \text{ such that }\quad \zeta_{\mathfrak{l},\nu}(k)\equiv h_{\mathfrak{l}}(\pi_{\mathfrak{l},\nu}(k+1))-h_{\mathfrak{l}}(\pi_{\mathfrak{l},\nu}(k)) \text{ mod } 2.$$

For $\mathfrak{s} \in \mathcal{S}$ and $(\pi, \zeta) \in \mathcal{BB}_{\mathfrak{s}}$, we denote by $\mathcal{L}_{\mathfrak{s},\nu}^{(\pi,\zeta)}$ the set of labeled schemes \mathfrak{l} such that us(\mathfrak{l}) = \mathfrak{s} and $(\pi_{\mathfrak{l},\nu}, \zeta_{\mathfrak{l},\nu}) = (\pi, \zeta)$. We denote by $\mathcal{R}_{\mathfrak{s},\nu}^{(\pi,\zeta)}$ the subset of elements of \mathcal{R} whose labeled scheme belongs to $\mathcal{L}_{\mathfrak{s},\nu}^{(\pi,\zeta)}$.

7.1.2. Binary bijections and the mirror operation. To be able to state an analogue of Lemma 6.1 in the bivariate case, we first introduce some refinements of $\mathcal{L}_{\mathfrak{s},\nu}^{(\pi,\zeta)}$. For $\mathfrak{l}\in\mathcal{L}_{\mathfrak{s},\nu}^{(\pi,\zeta)}$, we denote by $\overline{\mathfrak{l}}$ the labeled scheme obtained from \mathfrak{l} by shifting all its labels by 1, and we set $\overline{\mathcal{L}}_{\mathfrak{s},\nu}^{(\pi,\zeta)}=\{\overline{\mathfrak{l}}\,|\,\mathfrak{l}\in\mathcal{L}_{\mathfrak{s},\nu}^{(\pi,\zeta)}\}$. Note that for $\mathfrak{l}\in\mathcal{L}_{\mathfrak{s},\nu}^{(\pi,\zeta)}$, the parity of $h_{\overline{\mathfrak{l}}}(\pi^{-1}(1))$ is prescribed by ζ and if $h_{\overline{\mathfrak{l}}}(\pi^{-1}(1))$ is odd, then $h_{\overline{\mathfrak{l}}}(\pi^{-1}(1))$ is even and reciprocally. We then define:

(15)
$$\begin{cases} {}^{\bullet}\mathcal{L}_{\mathfrak{s},\nu}^{(\pi,\zeta):+} = \left\{ \mathfrak{l} \in \mathcal{L}_{\mathfrak{s},\nu}^{(\pi,\zeta)} \cup \overline{\mathcal{L}}_{\mathfrak{s},\nu}^{(\pi,\zeta)} \mid h_{\mathfrak{l}}(\pi^{-1}(1)) \text{ is odd} \right\} \\ {}^{\circ}\mathcal{L}_{\mathfrak{s},\nu}^{(\pi,\zeta):+} = \left\{ \mathfrak{l} \in \mathcal{L}_{\mathfrak{s},\nu}^{(\pi,\zeta)} \cup \overline{\mathcal{L}}_{\mathfrak{s},\nu}^{(\pi,\zeta)} \mid h_{\mathfrak{l}}(\pi^{-1}(1)) \text{ is even} \right\} \end{cases}$$

and, similarly:

(16)
$$\begin{cases} {}^{\bullet}\mathcal{L}_{\mathfrak{s},\nu}^{(\pi,\zeta):-} = \left\{ \mathfrak{l} \in \mathcal{L}_{\mathfrak{s},\nu}^{(\pi,\zeta)} \cup \overline{\mathcal{L}}_{\mathfrak{s},\nu}^{(\pi,\zeta)} \mid h_{\mathfrak{l}}\left(\pi^{-1}(|V(\mathfrak{s})|)\right) \text{ is odd} \right\} \\ {}^{\circ}\mathcal{L}_{\mathfrak{s},\nu}^{(\pi,\zeta):-} = \left\{ \mathfrak{l} \in \mathcal{L}_{\mathfrak{s},\nu}^{(\pi,\zeta)} \cup \overline{\mathcal{L}}_{\mathfrak{s},\nu}^{(\pi,\zeta)} \mid h_{\mathfrak{l}}\left(\pi^{-1}(|V(\mathfrak{s})|)\right) \text{ is even} \right\}. \end{cases}$$

Next, for $\pm \in \{-,+\}$, we define:

$$(17) \qquad {}^{\bullet}S_{\mathfrak{s},\nu}^{(\pi,\zeta):\pm}(D_{\bullet},D_{\circ}) = \sum_{\mathfrak{l}\in {}^{\bullet}\mathcal{L}^{(\pi,\zeta):\pm}} \left(\prod_{e\in E^{\uparrow}(\mathfrak{l})} \Delta_{\lambda_{\mathfrak{l}}^{0}(e)}^{\lambda_{\mathfrak{l}}^{1}(e)}(D_{\bullet},D_{\circ}) \prod_{e\in E^{\downarrow}(\mathfrak{l})} \Delta_{\lambda_{\mathfrak{l}}^{1}(e)}^{\lambda_{\mathfrak{l}}^{0}(e)}(D_{\circ},D_{\bullet}) \right).$$

and

$$(18) \qquad {}^{\circ}S_{\mathfrak{s},\nu}^{(\pi,\zeta):\pm}(D_{\bullet},D_{\circ}) = \sum_{\mathfrak{l}\in {}^{\circ}\mathcal{L}_{\mathfrak{s},\nu}^{(\pi,\zeta):\pm}} \left(\prod_{e\in E^{\uparrow}(\mathfrak{l})} \Delta_{\lambda_{\mathfrak{l}}^{0}(e)}^{\lambda_{\mathfrak{l}}^{1}(e)}(D_{\bullet},D_{\circ}) \prod_{e\in E^{\downarrow}(\mathfrak{l})} \Delta_{\lambda_{\mathfrak{l}}^{1}(e)}^{\lambda_{\mathfrak{l}}^{0}(e)}(D_{\circ},D_{\bullet}) \right).$$

We then extend the mirror operation to binary bijections. For $(\pi, \zeta) \in \mathcal{BB}_{\mathfrak{s}}$, we set:

(19)
$$\overline{\zeta}(k) = \zeta(|V(\mathfrak{s})| - k), \quad \text{for any} \quad k \in [|V(\mathfrak{s})| - 1],$$

and we define $\overline{(\pi,\zeta)} := (\overline{\pi},\overline{\zeta})$, where we recall the definition of $\overline{\pi}$ given in (11).

Lemma 7.1. Let $\mathfrak{s} \in \mathcal{S}$, ν be a consistent naming \mathfrak{s} and $(\pi, \zeta) \in \mathcal{BB}_{\mathfrak{s}}$. Then, we have the following equality of generating series:

$$\overline{\bullet S_{\mathfrak{s},\nu}^{(\pi,\zeta):+}}^{\parallel} = (-1)^{|V(\mathfrak{s})|-1} \cdot {}^{\circ}S_{\mathfrak{s},\nu}^{\overline{(\pi,\zeta)}:-} \qquad and \qquad \overline{{}^{\circ}S_{\mathfrak{s},\nu}^{(\pi,\zeta):+}}^{\parallel} = (-1)^{|V(\mathfrak{s})|-1} \cdot {}^{\bullet}S_{\mathfrak{s},\nu}^{\overline{(\pi,\zeta)}:-}$$

The proof of Lemma 7.1 is postponed to Section 7.3.3 and is obtained as a special case of Lemma 7.5. We first show how it enables to finish the proof of Theorem 5.11.

7.2. **Proof of Theorem 5.11.** Let $\mathfrak{s} \in \mathcal{S}$, ν a consistent naming of \mathfrak{s} , $(\pi, \zeta) \in \mathcal{BB}_{\mathfrak{s}}$ and $\mathfrak{l} \in \mathcal{L}_{\mathfrak{s}, \nu}^{(\pi, \zeta)}$. By Lemma 5.4:

$$R_{\mathfrak{l}}(D_{\bullet},D_{\circ}) = B^{|E(\mathfrak{l})|} \cdot \prod_{r \in \mathcal{S}^{\rho}(\mathfrak{l})} \Delta_{\lambda_{\mathfrak{l}}(r)}^{\lambda_{\mathfrak{l}}(r)+1}(t_{\bullet},t_{\circ}) \cdot \prod_{e \in E^{\uparrow}(\mathfrak{l})} \Delta_{\lambda_{\mathfrak{l}}^{0}(e)}^{\lambda_{\mathfrak{l}}^{1}(e)}(D_{\bullet},D_{\circ}) \cdot \prod_{e \in E^{\downarrow}(\mathfrak{l})} \Delta_{\lambda_{\mathfrak{l}}^{1}(e)}^{\lambda_{\mathfrak{l}}^{0}(e)}(D_{\circ},D_{\bullet}).$$

We first compute the contribution of the rootable scheme stems of \mathfrak{l} . Recall Definition 5.17. For $r \in S^{\rho}(\mathfrak{l})$, if r is regular, then its relative label $\lambda_{\mathfrak{s}}(r)$ in \mathfrak{s} is equal to 1, and if r is shifted, then $\lambda_{\mathfrak{s}}(r) = 2$. Hence, any $r \in S^{\rho}(\mathfrak{l})$ contributes to a weight t_{\bullet} if $h_{\mathfrak{l}}(v(r)) + \lambda_{\mathfrak{s}}(r)$ is odd, and t_{\circ} otherwise.

Let $c \in \{\bullet, \circ\}$ be such that $\mathfrak{l} \in {}^{c}\mathcal{L}_{\mathfrak{s}, \nu}^{(\pi, \zeta):+}$ (observe that c takes the same value for any $\mathfrak{l} \in \mathcal{L}_{\mathfrak{s}, \nu}^{(\pi, \zeta)}$). Define $-c \in \{\bullet, \circ\}$ such that $\{c, -c\} = \{\bullet, \circ\}$, i.e. -c is the opposite color of c. Then, the contribution of the scheme rootable stems of \mathfrak{l} , is given by

$${}^{c}\mathsf{P}_{\mathfrak{s},\nu}^{(\pi,\zeta):+} := \sum_{r \in \mathcal{S}^{\rho}(\mathfrak{s})} \begin{cases} t_{c}, & \text{if } \sum_{i=1}^{\pi^{-1}(\mathsf{v}(r)-1)} \zeta(i) \equiv \lambda_{\mathfrak{s}}(r) \text{ (mod 2)}, \\ t_{-c}, & \text{otherwise.} \end{cases}$$

Hence:

$$R_{\mathfrak{l}}(D_{\bullet},D_{\circ}) = {^{c}\mathsf{P}}_{\mathfrak{s},\nu}^{(\pi,\zeta):+} \cdot B^{|E(\mathfrak{l})|} \cdot \left(\prod_{e \in E^{\uparrow}(\mathfrak{l})} \Delta_{\lambda_{\mathfrak{l}}^{0}(e)}^{\lambda_{\mathfrak{l}}^{1}(e)}(D_{\bullet},D_{\circ}) \prod_{e \in E^{\downarrow}(\mathfrak{l})} \Delta_{\lambda_{\mathfrak{l}}^{1}(e)}^{\lambda_{\mathfrak{l}}^{0}(e)}(D_{\circ},D_{\bullet}) \right),$$

from which it follows:

$$R_{\mathfrak{s},\nu}^{(\pi,\zeta)}(D_{\bullet},D_{\circ}) = {}^{c}P_{\mathfrak{s},\nu}^{(\pi,\zeta):+} \cdot B^{|E(\mathfrak{s})|} \cdot {}^{c}S_{\mathfrak{s},\nu}^{(\pi,\zeta):+}.$$

Next, recall the expressions of t_{\bullet} and t_{\circ} given in (7) and (8) and of B given in (9) and observe that:

$$t_{\bullet}(D_{\circ}, D_{\bullet}) = t_{\circ}(D_{\bullet}, D_{\circ})$$
 and $B(D_{\bullet}, D_{\circ}) = B(D_{\circ}, D_{\bullet}),$

and therefore, we have:

$$R_{\mathfrak{s},\nu}^{(\pi,\zeta)}(D_{\circ},D_{\bullet}) = {}^{-c}P_{\mathfrak{s},\nu}^{(\pi,\zeta):+} \cdot B^{|E(\mathfrak{s})|} \cdot {}^{-c}S_{\mathfrak{s},\nu}^{(\pi,\zeta):+},$$

and

$$\left(R_{\mathfrak{s},\nu}^{(\pi,\zeta)}\right)^{\bullet} = B^{|E(\mathfrak{s})|} \cdot \left({}^{\circ}\mathrm{P}_{\mathfrak{s},\nu}^{(\pi,\zeta):+} \cdot {}^{\circ}S_{\mathfrak{s},\nu}^{(\pi,\zeta):+} + {}^{\bullet}\mathrm{P}_{\mathfrak{s},\nu}^{(\pi,\zeta):+} \cdot {}^{\bullet}S_{\mathfrak{s},\nu}^{(\pi,\zeta):+} \right)$$

Following the same chain of arguments, we can also obtain the following equivalent expression:

$$\left(R_{\mathfrak{s},\nu}^{(\pi,\zeta)}\right)^{\bullet} = B^{|E(\mathfrak{s})|} \cdot \left({}^{\circ}P_{\mathfrak{s},\nu}^{(\pi,\zeta):-} \cdot {}^{\circ}S_{\mathfrak{s},\nu}^{(\pi,\zeta):-} + {}^{\bullet}P_{\mathfrak{s},\nu}^{(\pi,\zeta):-} \cdot {}^{\bullet}S_{\mathfrak{s},\nu}^{(\pi,\zeta):-} \right),$$

where, for $c \in \{\bullet, \circ\}$, we set:

$${}^{c}\mathsf{P}_{\mathfrak{s},\nu}^{(\pi,\zeta):-} := \sum_{r \in \mathcal{S}^{\rho}(\mathfrak{s})} \begin{cases} t_{c}, & \text{if } \sum_{i=\pi^{-1}(\mathbf{v}(r))}^{|V(\mathfrak{s})|-1} \zeta(i) \equiv \lambda_{\mathfrak{s}}(r) \pmod{2}, \\ t_{-c}, & \text{otherwise.} \end{cases}$$

We can finally compute $\overline{\left(R_{\mathfrak{s},\nu}^{(\pi,\zeta)}\right)^{\mathfrak{O}}}^{\parallel}$ and write:

$$\overline{\left(R_{\mathfrak{s},\nu}^{(\pi,\zeta)}\right)^{\bullet}}^{\parallel} = \overline{B^{|E(\mathfrak{s})|} \cdot \left({}^{\circ} \mathtt{P}_{\mathfrak{s},\nu}^{(\pi,\zeta):+} \cdot {}^{\circ} S_{\mathfrak{s},\nu}^{(\pi,\zeta):+} + {}^{\bullet} \mathtt{P}_{\mathfrak{s},\nu}^{(\pi,\zeta):+} \cdot {}^{\bullet} S_{\mathfrak{s},\nu}^{(\pi,\zeta):+} \right)^{\parallel}}$$

From (9), it is easy to see that $\overline{B}^{\parallel} = -B$. Similarly from (8) and (7), we have $\overline{t_{\circ}}^{\parallel} = t_{\bullet}$ and $\overline{t_{\bullet}}^{\parallel} = t_{\circ}$, so that $\overline{c_{\mathsf{p}}^{(\pi,\zeta)}} = {}^{-c}\mathrm{p}_{\mathfrak{s},\nu}^{(\overline{\pi,\zeta})}$. By Lemma 7.5, we hence get:

$$\overline{\left(R_{\mathfrak{s},\nu}^{(\pi,\zeta)}\right)^{\bullet}}^{\parallel} = (-1)^{|E(\mathfrak{s})| + |V(\mathfrak{s})| - 1} \cdot B^{|E(\mathfrak{s})|} \cdot \left(^{\bullet} \mathbf{P}_{\mathfrak{s},\nu}^{\overline{(\pi,\zeta)}:-} \cdot ^{\bullet} S_{\mathfrak{s},\nu}^{\overline{(\pi,\zeta)}:-} + ^{\circ} \mathbf{P}_{\mathfrak{s},\nu}^{\overline{(\pi,\zeta)}:-} \cdot ^{\circ} S_{\mathfrak{s},\nu}^{\overline{(\pi,\zeta)}:-}\right)$$

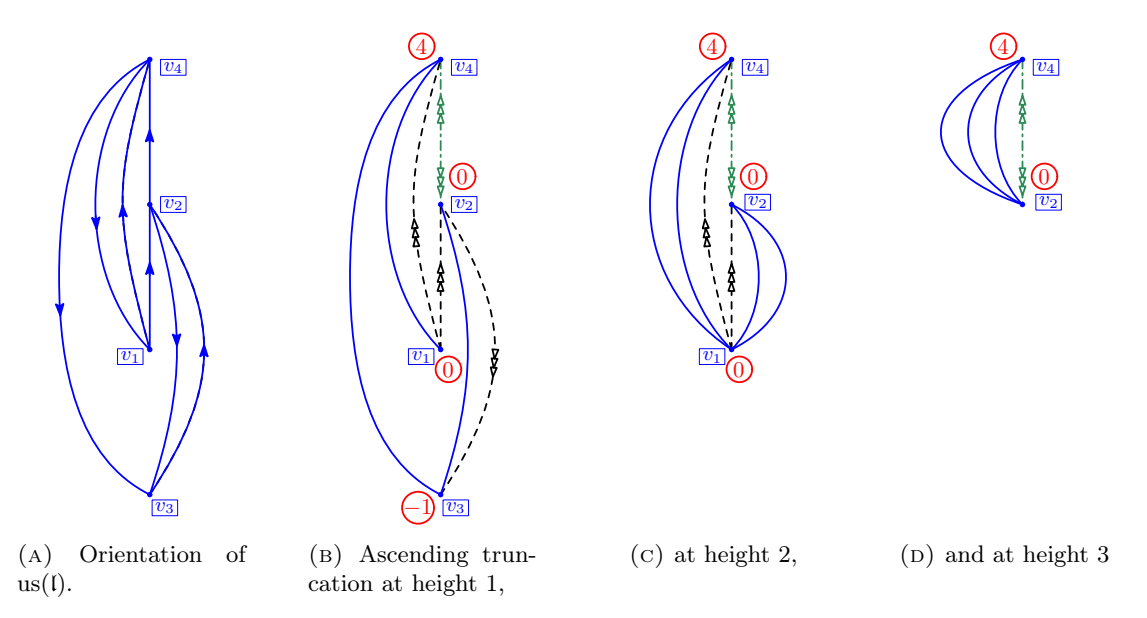


FIGURE 18. We still consider the labeled scheme of Figure 16(A), with the same naming ν . In (A), we represent as a graph the interior map of its unlabeled scheme. The ordering (from bottom to top) of its vertices is given by its height order relative to ν . The orientation of its edges corresponds to the canonical orientation of \mathfrak{l} .

In (B), (C) and (D), we represent respectively the ascending truncation of $\mathfrak l$ at height 1, 2 and 3. For sake of clarity, we do not represent the projection of the canonical orientation of $\mathfrak l$ on its truncations. But, it can hopefully be deduced from (A).

and, by (20):

$$\overline{\left(R_{\mathfrak{s},\nu}^{(\pi,\zeta)}\right)^{\mathfrak{C}}}^{\parallel} = (-1)^{|E(\mathfrak{s})|+|V(\mathfrak{s})|-1} \cdot \left(R_{\mathfrak{s},\nu}^{\overline{(\pi,\zeta)}}\right)^{\mathfrak{C}}.$$

By Euler's formula, for any unlabeled scheme, we have $|E(\mathfrak{s})|+|V(\mathfrak{s})|-1=2g$. And, since

$$\left(R_{\mathfrak{s},\nu}^{\pi}\right)^{\bullet} = \sum_{\zeta:[|V(\mathfrak{s})|-1]\to\mathbb{Z}/2\mathbb{Z}} \left(R_{\mathfrak{s},\nu}^{(\pi,\zeta)}\right)^{\bullet},$$

this concludes the proof.

7.3. Proof of Lemma 7.1 via truncations.

7.3.1. Truncations. In all this section, we fix $\mathfrak{s} \in \mathcal{S}$ and ν a consistent naming of \mathfrak{s} .

Definition 7.2. For $\mathfrak{l} \in \mathcal{L}_{\mathfrak{s},\nu} \cup \bar{\mathcal{L}}_{\mathfrak{s},\nu}$ and $k \in [|V(\mathfrak{l})|]$, the ascending truncation of \mathfrak{l} at relative height k – denoted $\Pi^{k:+}(\mathfrak{l})$ – is the oriented and labeled graph, with typed half-edges, obtained as follows, see Figure 18.

Start with \mathfrak{l} endowed with its canonical orientation, and label its vertices by their height. Consider the subset X of vertices of \mathfrak{l} defined by $X = \pi_{\mathfrak{l},\nu}([k-1])$, then:

- Delete all the stems of \mathfrak{l} .
- Set to 0 the type of all the half-edges adjacent to vertices of X (i.e. replace offset edges towards a vertex of X and shifted edges between two vertices of X by balanced edges, and shifted edges between $u \in X$ and $v \notin X$ by an offset edge towards v).
- Finally, merge all the vertices of X with $\pi_{\mathfrak{l},\nu}(k)$, label this vertex $h_{\mathfrak{l}}(\pi_{\mathfrak{l},\nu}(k))$, and erase the self-loops thus created.

We define similarly the descending truncation of \mathfrak{l} at relative height k – denoted by $\Pi^{k:-}(\mathfrak{l})$ – by setting instead $X = \pi_{\mathfrak{l},\nu}([k,|V(\mathfrak{s})|])$ in the previous construction.

We now introduce the set of graphs that can be obtained as the truncation of a labeled scheme.

Definition 7.3. For $(\pi, \zeta) \in \mathcal{BB}_{\mathfrak{s}}$, $k \in |V(\mathfrak{s})|$, and $\pm \in \{-, +\}$ we denote by:

$${}^{\circ}\mathcal{T}_{\mathfrak{s},\nu}^{(\pi,\zeta),k:\pm} = \left\{ \Pi^{k,\pm}(\mathfrak{l}) \, | \, \mathfrak{l} \in \mathcal{L}_{\mathfrak{s},\nu}^{(\pi,\zeta)} \, \cup \bar{\mathcal{L}}_{\mathfrak{s},\nu}^{(\pi,\zeta)} \, \, \text{such that } h_{\mathfrak{l}}(\pi(k)) \, \, \text{is even} \right\},$$

and

$${}^{\bullet}\mathcal{T}^{(\pi,\zeta),k:\pm}_{\mathfrak{s},\nu} = \left\{ \Pi^{k,\pm}(\mathfrak{l}) \, | \, \mathfrak{l} \in \mathcal{L}^{(\pi,\zeta)}_{\mathfrak{s},\nu} \cup \bar{\mathcal{L}}^{(\pi,\zeta)}_{\mathfrak{s},\nu} \ such \ that \ h_{\mathfrak{l}}(\pi(k)) \ is \ odd \right\}.$$

Additionally, we denote by $\mathcal{T}_{\mathfrak{s},\nu}^{(\pi,\zeta)}$ the set of all truncations, i.e.

$$\mathcal{T}_{\mathfrak{s},\nu}^{(\pi,\zeta)} = \bigcup_{\substack{k \in |V(\mathfrak{s})|, \pm \in \{-,+\}, c \in \{\bullet, \circ\}}} {}^{c}\mathcal{T}_{\mathfrak{s},\nu}^{(\pi,\zeta),k:\pm}.$$

Vertices of a truncation inherit naturally the height of the vertices of their preimage. For $\mathfrak{t} \in \mathcal{T}_{\mathfrak{s},\nu}^{(\pi,\zeta)}$ and $v \in V(\mathfrak{t})$, by a slight abuse of notation we still denote by $h_{\mathfrak{t}}(v)$ this value. We now extend consistently the definition of $\lambda^0(e)$ and $\lambda^1(e)$ for $e \in E(\mathfrak{t})$ in the following way. Fix first $\mathfrak{l} \in \mathcal{L}_{\mathfrak{s},\nu} \cup \bar{\mathcal{L}}_{\mathfrak{s},\nu}$. For $e = \{u_0, u_1\} \in E(\mathfrak{l})$ oriented from u_0 to u_1 , for $k \in [|V(\mathfrak{l})|]$, and for $\varepsilon \in \{0, 1\}$, we define:

$$\lambda_{\mathfrak{l}}^{\varepsilon,k:+}(e) = \begin{cases} h_{\mathfrak{l}}(\pi(k)), & \text{if } \pi^{-1}(u_{\varepsilon}) < k \text{ or if } \pi^{-1}(u_{\varepsilon}) = k \text{ and } \pi^{-1}(u_{1-\varepsilon}) < k, \\ \lambda_{\mathfrak{l}}^{\varepsilon}(e), & \text{otherwise.} \end{cases}$$

and

$$\lambda_{\mathfrak{l}}^{\varepsilon,k:-}(e) = \begin{cases} h_{\mathfrak{l}}(\pi(k)), & \text{if } \pi^{-1}(u_{\varepsilon}) > k \text{ or if } \pi^{-1}(u_{\varepsilon}) = k \text{ and } \pi^{-1}(u_{1-\varepsilon}) > k, \\ \lambda_{\mathfrak{l}}^{\varepsilon}(e), & \text{otherwise.} \end{cases}$$

For $k \in [|V(\mathfrak{s})|]$, let $\mathfrak{l}_1, \mathfrak{l}_2 \in \mathcal{L}_{\mathfrak{s},\nu}^{(\pi,\zeta)} \cup \bar{\mathcal{L}}_{\mathfrak{s},\nu}^{(\pi,\zeta)}$ be such that $\Pi^{k:+}(\mathfrak{l}_1) = \Pi^{k:+}(\mathfrak{l}_2)$, and denote \mathfrak{t} their common truncation. Note that, for any edge e, $\lambda_{\mathfrak{l}_1}^{\varepsilon,k:+}(e) = \lambda_{\mathfrak{l}_2}^{\varepsilon,k:+}(e)$. We then define $\lambda_{\mathfrak{t}}^{\varepsilon}(e)$ as this common value. Similarly, if $\mathfrak{t} = \Pi^{k:-}(\mathfrak{l}_1) = \Pi^{k:-}(\mathfrak{l}_2)$, we set $\lambda_{\mathfrak{t}}^{\varepsilon}(e) := \lambda_{\mathfrak{l}_1}^{\varepsilon,k:-}(e) = \lambda_{\mathfrak{l}_2}^{\varepsilon,k:-}(e)$.

The definition of E^{\uparrow} and E^{\downarrow} first given in Section 5.1 can then also be naturally extended to truncations and for $\mathfrak{t} \in \mathcal{T}^{(\pi,\zeta)}_{\mathfrak{s},\nu}$:

$$E^{\uparrow}(\mathfrak{t}) = \left\{ e \in E(\mathfrak{t}) \, | \, \lambda^0_{\mathfrak{t}}(e) \leq \lambda^1_{\mathfrak{t}}(e) \right\} \quad \text{and} \quad E^{\downarrow}(\mathfrak{t}) = \left\{ e \in E(\mathfrak{t}) \, | \, \lambda^0_{\mathfrak{t}}(e) > \lambda^1_{\mathfrak{t}}(e) \right\}.$$

For $k \in [|V(\mathfrak{s})|], c \in \{\bullet, \circ\}$ and $\pm \in \{-, +\}$, we finally define:

$$(21) cS_{\mathfrak{s},\nu}^{(\pi,\zeta),k:\pm}(D_{\bullet},D_{\circ}) = \sum_{\mathfrak{t}\in c\mathcal{T}_{\mathfrak{s},\nu}^{(\pi,\zeta),k:\pm}} \left(\prod_{e\in E^{\uparrow}(\mathfrak{t})} \Delta_{\iota_{\mathfrak{t}}^{0}(e)}^{\lambda_{\mathfrak{t}}^{1}(e)}(D_{\bullet},D_{\circ}) \prod_{e\in E^{\downarrow}(\mathfrak{t})} \Delta_{\lambda_{\mathfrak{t}}^{1}(e)}^{\lambda_{\mathfrak{t}}^{0}(e)}(D_{\circ},D_{\bullet}) \right).$$

7.3.2. Recursive decomposition of truncations. For any $k \in |V(\mathfrak{s})|$, we partition the set of edges of \mathfrak{s} positively enclosing height k (see Definition 5.15) into $E_{\mathfrak{s},\nu}^{\pi,k,\uparrow}$ and $E_{\mathfrak{s},\nu}^{\pi,k,\downarrow}$, depending on whether they are increasing or decreasing. More precisely, for $e = \{u,v\} \in E(\mathfrak{s})$ oriented from u to v, we set:

$$\begin{cases} e \in E_{\mathfrak{s},\nu}^{\pi,k,\uparrow} & \text{if } \pi^{-1}(u) \le k < \pi^{-1}(v) \\ e \in E_{\mathfrak{s},\nu}^{\pi,k,\downarrow} & \text{if } \pi^{-1}(v) \le k < \pi^{-1}(u). \end{cases}$$

Recall from Definition 5.15 that $C^{\pi,k:+}_{\mathfrak{s},\nu} = |E^{\pi,k,\uparrow}_{\mathfrak{s},\nu}| + |E^{\pi,k,\downarrow}_{\mathfrak{s},\nu}|$. For $c \in \{\bullet,\circ\}$, $\pm \in \{+,-\}$ and for $\mathfrak{t} \in {}^{c}\mathcal{T}^{(\pi,\zeta),k:\pm}_{\mathfrak{s},\nu}$, by a slight abuse of notations, we identify elements of $E^{\pi,\ell,\uparrow}_{\mathfrak{s},\nu}$ and of $E^{\pi,\ell,\uparrow}_{\mathfrak{s},\nu}$ with their image in $E(\mathfrak{t})$, for any $\ell \in \{k,\ldots,|V(\mathfrak{s})|-1\}$.

Recall the definitions of $\delta_{\mathfrak{s},\nu}^{\pi,k:+}$ given in (12) and of $\mathfrak{of}_{\mathfrak{s}}^{\pi,k}(e)$ and $\mathfrak{uf}_{\mathfrak{s}}^{\pi,k}(e)$ given in Definition 5.16. For $e \in E(\mathfrak{s})$ and $k \in [|V(\mathfrak{s})|]$, we define the following functions:

$$W_{\mathfrak{s},\nu,e}^{\pi,0,k}(x,y) \coloneqq (xy)^{\delta_{\mathfrak{s},\nu}^{\pi,k:+}} \cdot \frac{x^{\mathrm{of}_{\mathfrak{s}}^{\pi,(k+1)}(e)}}{x^{\mathrm{uf}_{\mathfrak{s}}^{\pi,k}(e)}},$$

$$W^{\pi,1,k}_{\mathfrak{s},\nu,e}(x,y)\coloneqq x\cdot \frac{y^{\mathrm{of}^{\pi,(k+1)}_{\mathfrak{s}}(e)}}{x^{\mathrm{uf}^{\pi,k}_{\mathfrak{s}}(e)}}.$$

And, finally for $c \in \{\bullet, \circ\}$, we introduce:

$${}^{c}W_{\mathfrak{s},\nu,e}^{(\pi,\zeta),k}(D_{\bullet},D_{\circ}) \coloneqq \begin{cases} W_{\mathfrak{s},\nu,e}^{\pi,\zeta(k),k}(D_{-c},D_{c}), & \text{if } e \in E_{\mathfrak{s},\nu}^{\pi,k,\uparrow}, \\ W_{\mathfrak{s},\nu,e}^{\pi,\zeta(k),k}(D_{c},D_{-c}), & \text{if } e \in E_{\mathfrak{s},\nu}^{\pi,k,\downarrow}, \\ 1, & \text{otherwise.} \end{cases}$$

Lemma 7.4. For $\mathfrak{s} \in \mathcal{S}$, ν a consistent naming of \mathfrak{s} and for $(\pi, \zeta) \in \mathcal{BB}_{\mathfrak{s}}$, the family of functions $\left({}^{c}S_{\mathfrak{s},\nu}^{(\pi,\zeta),k:\pm}, \text{ with } \pm \in \{-,+\}, c \in \{\bullet,\circ\}, k \in [|V(\mathfrak{s})|]\right)$ admits the following recursive characterization. For any $c \in \{\bullet,\circ\}$:

$${}^{c}S_{\mathfrak{s},\nu}^{(\pi,\zeta),|V(\mathfrak{s})|:+}=1, \quad and \quad {}^{c}S_{\mathfrak{s},\nu}^{(\pi,\zeta),1:-}=1,$$

Moreover, for any $k \in [|V(\mathfrak{s}) - 1|]$, we have:

$${}^{c}S_{\mathfrak{s},\nu}^{(\pi,\zeta),k:+} = \frac{\prod\limits_{e \in E(\mathfrak{s})} {}^{c}W_{\mathfrak{s},\nu,e}^{(\pi,\zeta),k}}{1 - (D_{\mathfrak{o}}D_{\bullet})^{\mathsf{C}_{\mathfrak{s}}^{\pi,k}}} \cdot ^{\left((-1)^{\zeta(k)}c\right)}S_{\mathfrak{s},\nu}^{(\pi,\zeta),(k+1):+}.$$

and,

$$^{c}S_{\mathfrak{s},\nu}^{(\pi,\zeta),k+1:-} = \frac{\prod\limits_{e \in E(\mathfrak{s})}^{\left((-1)^{\zeta(k)}c\right)}W_{\mathfrak{s},\nu,e}^{(\pi,\zeta),k}}{1 - (D_{\circ}D_{\bullet})^{\mathfrak{C}_{\mathfrak{s}}^{\pi,k}}} \cdot {}^{\left((-1)^{\zeta(k)}c\right)}S_{\mathfrak{s},\nu}^{(\pi,\zeta),k:-}.$$

Proof. From the definition of ascending and descending truncation, for $c \in \{\bullet, \circ\}$, the sets ${}^c\mathcal{T}^{(\pi,\zeta),|V(\mathfrak{s})|:+}_{\mathfrak{s},\nu}$ and ${}^c\mathcal{T}^{(\pi,\zeta),1:-}_{\mathfrak{s},\nu}$ are all reduced to a single element with one vertex and no edge. The initialisation cases follow easily.

Fix now $k \in [|V(\mathfrak{s})|-1]$. For $\mathfrak{t} \in \mathcal{T}^{(\pi,\zeta),k:+}_{\mathfrak{s},\nu}$, we now investigate the contribution of any $e \in E(\mathfrak{t})$ to ${}^cS^{(\pi,\zeta),k:+}_{\mathfrak{s},\nu}$. If e positively encloses an height larger than k, then its contribution to ${}^cS^{(\pi,\zeta),k:+}_{\mathfrak{s},\nu}$ is the same as its contribution to ${}^{(-1)^{\zeta(k)}}{}^cS^{(\pi,\zeta),k+1:+}_{\mathfrak{s},\nu}$. We hence need to focus only on edges positively enclosing height k.

Suppose first that $e \in E_{\mathfrak{s},\nu}^{\pi,k,\uparrow}$. Since ν is a consistent naming of \mathfrak{s} , $\lambda_{\mathfrak{t}}^{0}(e) \leq h_{\mathfrak{t}}(\pi(k+1))$. Hence, its contribution can be split into two parts. The first part is given by $w_{1}(e) := \Delta_{\lambda_{\mathfrak{t}}^{0}(e)}^{h_{\mathfrak{t}}(\pi(k+1))}(D_{\bullet}, D_{\circ})$

and the second one by $w_2(e) := \Delta_{h_t(\pi(k+1))}^{\lambda_t^1(e)}(D_{\bullet}, D_{\circ})$. We focus first on the first part and set:

$$\Delta_k := h_{\mathfrak{l}}(\pi(k+1)) - h_{\mathfrak{l}}(\pi(k)).$$

Then if $\zeta(k) = 1$, Δ_k can be any positive odd integer and if $\zeta(k) = 0$, Δ_k can be any even integer not smaller than $\delta_{\mathfrak{s},\nu}^{\pi,k:+}$. Then, if the half-edge of e incident to $\pi(k)$ is of type 0, i.e. if $\lambda_{\mathfrak{t}}^{0}(e) = h_{\mathfrak{t}}(\pi(k))$, then:

$$w_1(e) = \begin{cases} (D_c D_{-c})^{\Delta_k/2} & \text{if } \Delta_k \in 2\mathbb{N} \\ D_{-c}(D_c D_{-c})^{(\Delta_k - 1)/2} & \text{if } \Delta_k \in 2\mathbb{N} + 1. \end{cases}$$

Otherwise, i.e. if e is underfitting at height k, we need to divide the above formula by $\Delta_{h_{\mathfrak{t}}(\pi(k))}^{\lambda_{\mathfrak{t}}^{0}(e)}$, which amounts to including a correction term equal to D_{-c}^{-1} . It gives:

$$w_1(e) = \begin{cases} (D_c D_{-c})^{\Delta_k/2} & \text{if } \Delta_k \in 2\mathbb{N} \\ D_{-c}(D_c D_{-c})^{(\Delta_k - 1)/2} & \text{if } \Delta_k \in 2\mathbb{N} + 1. \end{cases}$$

We now move the evaluation of $w_2(e)$. If e is overfitting at height k+1, then:

$$w_2(e) = \begin{cases} D_c & \text{if } \zeta(k) = 1, \\ D_{-c} & \text{if } \zeta(k) = 0. \end{cases}$$

Otherwise, $w_2(e)$ is exactly equal to the contribution to ${}^{(-1)^{\zeta(k)}c}S_{\mathfrak{s},\nu}^{(\pi,\zeta),k+1:+}$ of the image of e in $\Pi^{k+1,:}(\mathfrak{t})$.

If $e \in E_{\mathfrak{s},\nu}^{\pi,k,\downarrow}$, the exact same analysis can be carried out except that we need to exchange c and -c in all the expressions obtained above. Summarizing all the contribution of edges of \mathfrak{t} , and summing over \mathfrak{t} , and over all possible values of Δ_k we get:

For $\zeta(k) = 1$:

$$\begin{split} \frac{cS_{\mathfrak{s},\nu}^{(\pi,\zeta),k:+}}{(-c)S_{\mathfrak{s},\nu}^{(\pi,\zeta),(k+1):+}} &= \sum_{i\geq 0} \left(\prod_{e\in E_{\mathfrak{s},\nu}^{\pi,k,\uparrow}} \frac{D_{-c}(D_{\circ}D_{\bullet})^{i}(D_{c})^{\mathsf{of}_{\mathfrak{s}}^{\pi,k+1}(e)}}{D_{-c}^{\mathsf{uf}_{\mathfrak{s}}^{\pi,k}(e)}} \cdot \prod_{e\in E_{\mathfrak{s},\nu}^{\pi,k,\downarrow}} \frac{D_{c}(D_{\circ}D_{\bullet})^{i}(D_{-c})^{\mathsf{of}_{\mathfrak{s}}^{\pi,k+1}(e)}}{D_{c}^{\mathsf{uf}_{\mathfrak{s}}^{\pi,k}(e)}} \right) \\ &= \prod_{e\in E_{\mathfrak{s},\nu}^{\pi,k,\uparrow}} \frac{D_{-c}(D_{c})^{\mathsf{of}_{\mathfrak{s}}^{\pi,k+1}(e)}}{(D_{-c})^{\mathsf{uf}_{\mathfrak{s}}^{\pi,k}(e)}} \cdot \prod_{e\in E_{\mathfrak{s},\nu}^{\pi,k,\downarrow}} \frac{D_{c}(D_{-c})^{\mathsf{of}_{\mathfrak{s}}^{\pi,k+1}(e)}}{(D_{c})^{\mathsf{uf}_{\mathfrak{s}}^{\pi,k}(e)}} \cdot \sum_{i\geq 0} \left((D_{\circ}D_{\bullet})^{\mathsf{c}_{\mathfrak{s}}^{\pi,k}} \right)^{i} \\ &= \prod_{e\in E(\mathfrak{s})} {}^{c}W_{\mathfrak{s},\nu,e}^{(\pi,\zeta),k}(D_{-c},D_{c})} \\ &= \frac{\prod_{e\in E(\mathfrak{s})} {}^{c}W_{\mathfrak{s},\nu,e}^{(\pi,\zeta),k}(D_{-c},D_{c})}}{1 - (D_{\circ}D_{\bullet})^{\mathsf{c}_{\mathfrak{s}}^{\pi,k}}} \end{split}$$

For $\zeta(k) = 0$, recall that Δ_k can take any even value not smaller than $\delta_{\mathfrak{s},\nu}^{\pi,k:+}$. Hence:

$$\frac{{}^{c}S^{(\pi,\zeta),k:+}_{\mathfrak{s},\nu}}{{}^{c}S^{(\pi,\zeta),(k+1):+}_{\mathfrak{s},\nu}} = \sum_{i \geq \delta^{\pi,k:+}_{\mathfrak{s},\nu}} \left(\prod_{e \in E^{\pi,k,\uparrow}_{\mathfrak{s},\nu}} \frac{(D_{\circ}D_{\bullet})^{i}(D_{-c})^{\circ \mathbf{f}^{\pi,k+1}_{\mathfrak{s}}(e)}}{D^{\mathsf{uf}^{\pi,k}_{\mathfrak{s}}(e)}_{-c}} \cdot \prod_{e \in E^{\pi,k,\downarrow}_{\mathfrak{s},\nu}} \frac{(D_{\circ}D_{\bullet})^{i}(D_{c})^{\circ \mathbf{f}^{\pi,k+1}_{\mathfrak{s}}(e)}}{D^{\mathsf{uf}^{\pi,k}_{\mathfrak{s}}(e)}_{c}} \right)$$

$$= \frac{\prod_{e \in E(\mathfrak{s})} {}^{c}W^{(\pi,\zeta),k}_{\mathfrak{s},\nu,e}}{1 - (D_{\circ}D_{\bullet})^{c^{\pi,k}_{\mathfrak{s}}}}$$

As a consequence, we obtain the recurrence relation:

$${}^{c}S_{\mathfrak{s},\nu}^{(\pi,\zeta),k:+} = \frac{\prod\limits_{e \in E(\mathfrak{s})} {}^{c}W_{\mathfrak{s},\nu,e}^{(\pi,\zeta),k}}{1 - (D_{\circ}D_{\bullet})^{\mathsf{C}_{\mathfrak{s}}^{\pi,k}}} \cdot {}^{((-1)^{\zeta(k)}c)}S_{\mathfrak{s},\nu}^{(\pi,\zeta),(k+1):+}.$$

The other recurrence relation (for descending truncation) is obtained similarly.

7.3.3. Mirror operation and truncations. Recall (15) and (16). Since ${}^{c}\mathcal{T}_{\mathfrak{s},\nu}^{(\pi,\zeta),1:+} = {}^{c}\mathcal{L}_{\mathfrak{s},\nu}^{(\pi,\zeta):+}$ and ${}^{c}\mathcal{T}_{\mathfrak{s},\nu}^{(\pi,\zeta),|V(\mathfrak{s})|:-} = {}^{c}\mathcal{L}_{\mathfrak{s},\nu}^{(\pi,\zeta):-}$, the definition of ${}^{c}S_{\mathfrak{s},\nu}^{(\pi,\zeta),k:\pm}$ given in (21) is a generalization of ${}^{\bullet}S_{\mathfrak{s},\nu}^{(\pi,\zeta):\pm}$ and ${}^{\circ}S_{\mathfrak{s},\nu}^{(\pi,\zeta):\pm}$ as defined in (17) and (18). Lemma 7.1 is then a direct corollary of the following more general result:

Lemma 7.5. Let $(\pi, \zeta) \in \mathcal{BB}_{\mathfrak{s}}$. Then, for any $k \in [|V(\mathfrak{s})|]$, we have:

$$\overline{cS_{\mathfrak{s},\nu}^{(\pi,\zeta),k:-}}^{\parallel} = (-1)^{k-1} \cdot {}^{-c}S_{\mathfrak{s},\nu}^{\overline{(\pi,\zeta)},\overline{k}:+}$$

where we recall that $\overline{k} = |V(\mathfrak{s})| + 1 - k$ and $\overline{(\pi, \zeta)}$ is defined in (19).

Proof. We start with an easy computation. For $k \in [|V(\mathfrak{s})|-1]$, by Proposition 5.18, we have:

$$(22) W_{\mathfrak{s},\nu,e}^{\pi,1,k}(x,y) \cdot W_{\mathfrak{s},\nu,e}^{\overline{\pi},1,\overline{k+1}}(y,x) = x \cdot \frac{y^{\text{of}_{\mathfrak{s}}^{\pi,(k+1)}(e)}}{x^{\text{uf}_{\mathfrak{s}}^{\pi,k}(e)}} \cdot y \cdot \frac{x^{\text{of}_{\mathfrak{s}}^{\pi,\bar{k}}(e)}}{y^{\text{uf}_{\mathfrak{s}}^{\pi,(k+1)}(e)}} = xy,$$

and

$$(23) W_{\mathfrak{s},\nu,e}^{\pi,0,k}(x,y) \cdot W_{\mathfrak{s},\nu,e}^{\overline{\pi},0,\overline{k+1}}(x,y) = (xy)^{\delta_{\mathfrak{s},\nu}^{\pi,k++}} \cdot \frac{x^{\mathrm{of}_{\mathfrak{s}}^{\pi,(k+1)}(e)}}{x^{\mathrm{uf}_{\mathfrak{s}}^{\pi,k}(e)}} \cdot (xy)^{\delta_{\mathfrak{s},\nu}^{\overline{\pi},\overline{k}-1++}} \cdot \frac{x^{\mathrm{of}_{\mathfrak{s}}^{\overline{\pi},\overline{k}}(e)}}{x^{\mathrm{uf}_{\mathfrak{s}}^{\overline{\pi},(\overline{k+1})}(e)}} = xy.$$

Next, observe that, for any $k \in [|V(\mathfrak{s})|]$:

$$\overline{{}^cW^{(\pi,\zeta),k}_{\mathfrak{s},\nu,e}}^{\|}(D_{\bullet},D_{\circ}) = \left({}^cW^{(\pi,\zeta),k}_{\mathfrak{s},\nu,e}(D_{\bullet},D_{\circ})\right)^{-1}.$$

Moreover, for $k \in [2, |V(\mathfrak{s})|]$, $E_{\mathfrak{s},\nu}^{\pi,k,\uparrow} = E_{\mathfrak{s},\nu}^{\overline{\pi},\overline{k+1},\downarrow}$, $E_{\mathfrak{s},\nu}^{\pi,k,\downarrow} = E_{\mathfrak{s},\nu}^{\overline{\pi},\overline{k+1},\uparrow}$ and $\overline{\zeta}(\overline{k+1}) = \zeta(k)$. Hence, together with (22) and (23), it implies that, for any $e \in E_{\mathfrak{s},\nu}^{\pi,k,\downarrow} \cup E_{\mathfrak{s},\nu}^{\pi,k,\uparrow}$:

(24)
$$\overline{{}^{c}W_{\mathfrak{s},\nu,e}^{(\pi,\zeta),k}}^{\parallel} = \frac{\left((-1)^{\zeta(k)+1}c\right)W_{\mathfrak{s},\nu,e}^{(\pi,\zeta),\overline{k+1}}}{D_{\bullet}D_{\circ}}.$$

We now proceed to the proof of the result by induction on k. By Lemma 7.4, the case k = 1 holds. Fix k > 1, we apply Lemma 7.4 to write:

$$\overline{cS_{\mathfrak{s},\nu}^{(\pi,\zeta),k+1:-}}^{\|\varepsilon(-1)^{\zeta(k)}c} = \frac{\prod_{e \in E(\mathfrak{s})} \overline{((-1)^{\zeta(k)}c)} W_{\mathfrak{s},\nu,e}^{(\pi,\zeta),k}}^{(\pi,\zeta),k} \cdot \overline{((-1)^{\zeta(k)}c)} S_{\mathfrak{s},\nu}^{(\pi,\zeta),k:-}$$

By the recurrence hypothesis coupled with Proposition 5.18 and Equation (24), we get:

$$\overline{{}^{c}S_{\mathfrak{s},\nu}^{(\pi,\zeta),k+1:-}}^{\|C_{\mathfrak{s},\nu}(\pi,\zeta),\overline{k+1}} = (-1)^{k-1} \cdot \frac{\prod\limits_{e \in E(\mathfrak{s})} {}^{-c}W_{\mathfrak{s},\nu,e}^{(\pi,\zeta),\overline{k+1}}}{(D_{\bullet}D_{\circ})^{\mathtt{C}^{\pi,\overline{k+1}}} \left(1 - (D_{\circ}D_{\bullet})^{-\mathtt{C}^{\overline{\pi},\overline{k+1}}_{\mathfrak{s}}}\right)} \cdot {}^{((-1)^{(\zeta(k)+1)}c)}S_{\mathfrak{s},\nu}^{(\overline{\pi,\zeta}),\overline{k}:+},$$

and finally:

$$\overline{{}_{c}S_{\mathfrak{s},\nu}^{(\pi,\zeta),k+1:-}}^{(\pi,\zeta),k+1:-}\| = (-1)^k \cdot {}^{-c}S_{\mathfrak{s},\nu}^{\overline{(\pi,\zeta)},\overline{k+1}:+}$$

which concludes the proof.

References

- D. Arques, Une relation fonctionnelle nouvelle sur les cartes planaires pointées, J. Combin. Theory Ser. B 39 (1985), no. 1, 27–42.
- D. Arquès, Relations fonctionnelles et dénombrement des cartes pointées sur le tore, J. Combin. Theory Ser. B 43 (1987), no. 3, 253–274.
- 3. D. Arques and A. Giorgetti, Énumération des cartes pointées sur une surface orientable de genre quelconque en fonction des nombres de sommets et de faces, J. Combin. Theory Ser. B 77 (1999), no. 1, 1-24.
- E.A. Bender and E.R. Canfield, The asymptotic number of rooted maps on a surface, J. Combin. Theory Ser. A 43 (1986), no. 2, 244–257.
- 5. _____, The number of rooted maps on an orientable surface, J. Combin. Theory Ser. B 53 (1991), no. 2, 293-299.
- E.A. Bender, E.R. Canfield, and L.B Richmond, The asymptotic number of rooted maps on a surface.: II. Enumeration by vertices and faces, J. Combin. Theory Ser. A 63 (1993), no. 2, 318–329.
- S.R. Carrell and G. Chapuy, Simple recurrence formulas to count maps on orientable surfaces, J. Combin. Theory Ser. A 133 (2015), 58–75.
- 8. G. Chapuy, M. Marcus, and G. Schaeffer, A bijection for rooted maps on orientable surfaces, SIAM J. Discrete Math. 23 (2009), no. 3, 1587–1611.
- 9. R. Cori and B. Vauquelin, Planar maps are well labeled trees, Canad. J. Math. 33 (1981), no. 5, 1023-1042.
- M. Dolega and M. Lepoutre, Blossoming bijection for bipartite pointed maps and parametric rationality of general maps on any surface, arXiv preprint arXiv:2002.07238 (2020).
- 11. B. Eynard, Counting surfaces, vol. 70, Springer, 2011.
- 12. Ph. Flajolet and R. Sedgewick, Analytic combinatorics, Cambridge University press, 2009.
- S.K. Lando and A.K. Zvonkin, Graphs on surfaces and their applications. Appendix by Don B. Zagier., Springer, 2004.
- 14. M. Lepoutre, Blossoming bijection for higher-genus maps, J. Combin. Theory Ser. A 165 (2019), 187–224.
- B. Lévêque, Generalization of Schnyder woods to orientable surfaces and applications, Habilitation à diriger des recherches, Université Grenoble Alpes, 2017.
- $16. \ \ J.\ Propp,\ \textit{Lattice structure for orientations of graphs},\ arXiv\ preprint\ math/0209005\ (2002).$
- 17. G. Schaeffer, Bijective census and random generation of Eulerian planar maps with prescribed vertex degrees, Electron. J. Combin. 4 (1997), no. 1, 20.
- 18. _____, Conjugaison d'arbres et cartes combinatoires aléatoires, Ph.D. thesis, Bordeaux 1, 1998.
- 19. _____, Planar Maps, Handbook of Enumerative Combinatorics (M Bóna, ed.), vol. 87, CRC Press, 2015.
- 20. W.T. Tutte, A census of slicings, Canad. J. Math. 14 (1962), 708–722.
- 21. _____, A census of planar maps, Canad. J. Math. 15 (1963), 249–271.
- 22. T. Walsh and A. Lehman, Counting rooted maps by genus. I, J. Combin. Theory Ser. B 13 (1972), no. 3, 192–218.
- 23. ______, Counting rooted maps by genus II, J. Combin. Theory Ser. B 13 (1972), no. 2, 122–141.

LIX UMR7161, École Polytechnique, 91120 Palaiseau, France

E-mail address: albenque@lix.polytechnique.fr
URL: http://www.lix.polytechnique.fr/Labo/Marie.Albenque/

LIX UMR7161, ÉCOLE POLYTECHNIQUE, 91120 PALAISEAU, FRANCE $E\text{-}mail\ address:}$ mathias.lepoutre@lix.polytechnique.fr URL: http://www.lix.polytechnique.fr/Labo/Mathias.Lepoutre/